The Structure, Stratigraphy and Regional Correlations of the Bulgobac Falls Area, NW Tasmania.

Peter Buxton B.Sc.

UNIVERSITY OF TASMANIA

A research thesis submitted
in partial fulfilment of the degree
of Bachelor of Science with Honours

Department of Geology,
University of Tasmania,
November, 1997.

To Andrew
with thanks for your
help, support + encouragement
over the year. All the best
in Samsonville - for the
future in general.
Regards
Peter.

98-4132 OF

STRUCTURE,STRATIGRAPHY &
REGIONAL CORRELATIONS OF BULGOBAC
FALLS AREA-EL 24/95-ABERFOYLE

Abstract

The stratigraphy of the Mount Read Volcanics in western Tasmania is complex and difficult to correlate due to the complicated nature of the original relationships and subsequent extensive faulting. Placing local stratigraphic sequences into a regional context is vital to unravelling the overall stratigraphy. This thesis describes the geology of the Bulgobac Falls area from a structural and stratigraphic perspective and correlates the geology to local and regional stratigraphy.

Structurally, the Bulgobac Falls area is simple. The sequence forms part of the eastern arm of a regional NNE trending syncline. Bedding dips and faces west, and strikes NNE. Two cleavages are weakly developed and axial planar to folds that trend NW or NNE. These are related to D2 and D4 of the Tabberabberan Orogeny. No significant faulting was observed within the area.

The Bulgobac Falls area is part of the Western volcano-sedimentary sequences and is bounded to the east by an intrusive quartz-feldspar porphyry. Overlying this is a sedimentary sequence of course and fine grained turbidites deposited in a sub-aqueous environment, below storm wave base. At the base of the sequence is a calcareous volcaniclastic sandstone containing calcite clasts with abundant Mid-Cambrian trilobites. Above this is a series of course grained volcaniclastic sandstones interbedded with finer sandstones and mudstones. The sandstones are crystal-rich, initially with feldspar and pyroxene and minor quartz. Higher in the stratigraphy they become quartz-rich. The Bulgobac Falls sequence is correlated to the Tyndall Group based on this trend, together with the textural, mineralogical, and geochemical similarity. This places the Bulgobac Falls sequence in the upper portion of the Mount Charter Group, within the Mount Cripps Subgroup, which has previously been correlated to the Tyndall Group.

Basal Tyndall Group rocks and there correlates are distinguishable by their highly magnetic character. Local correlations and aeromagnetic data suggests the base of the Mount Cripps Subgroup is a part of the Bulgobac Falls sequence. This was determined to be at the first crystal-rich sandstone unit within the sequence based on its mineralogical and geochemical similarity to Tyndall Group rocks. The underlying calcareous unit is correlated to similar units within the Southwell Subgroup, which underlies the Mount

Cripps Subgroup within the Mount Charter Group. Significantly this unit is not highly magnetic, suggesting the use of magnetic data is not reliable in precise definition of the stratigraphy of the Tyndall Group. The low magnetic signature of this unit is related to alteration of magnetite.

The Bulgobac Falls sequence was also correlated to outcrop of the Mount Charter Group in the Pinnacles area to the south. The stratigraphy was shown to be continuous between the two areas based on their relative positions within the Mount Charter Group and aeromagnetic data.

Acknowledgments

A great many people have contributed to this work over the year. My particular thanks go to my supervisor Dr. Ron Berry, he has been immensely supportive of my work and a great source of wry humour, along with more than a little geological wisdom.

Aberfoyle Resources have been wonderful sponsors for this project. Their logistical support has smoothed my path through the year and their staff have been both friends and mentors. I would particularly like to thank Andrew McNeill who has provided unending support, shown enviable patience with me and has an enthusiasm for geology that can only inspire. Gary Cooper made my field work a lot more fun in some fairly trying conditions and Richard deBomford provided enthusiastic support behind the scenes. Thankyou all, I thoroughly enjoyed working with you.

The staff at the university are too numerous to mention in detail. I have enjoyed my time with you all and wish you well in the future. Particular thanks must go to Paul Kitto, Clive Burrett, Kathi Staite, Simon Stevens, Phil Robinson and Christine Higgins, all of whom have helped make this year a little easier.

To Ruth and Carol; you have been great housemates and wonderful friends in good times and bad. Thankyou and good luck with your future paths. I also thank my fellow students for their humour, advice and assistance, the best of luck to you all.

Finally I would like to offer my most heartfelt thanks to Sandra. You have been a wonderful source of support and encouragement even when your own world seemed to be falling apart. May the coming years pass more smoothly for us both.

Table of Contents

List of Figures

List of Tables

Chapter 1: Introduction

1.1 Background

The Bulgobac Falls area incorporates a sequence of volcaniclastic sandstones and mudstones of uncertain stratigraphic position. Recent work in and around the area (eg. Kirsner, 1992; McKibben, 1993) has led to tentative correlation of the local area to the Mount Charter Group. The study of the sequence within the Bulgobac Falls area will help to place the region into its correct stratigraphic context and so lead to greater understanding of the complex stratigraphic relationships that occur within the Mount Read Volcanics.

1.2 Location and Access

The Bulgobac Falls are located approximately 10 km. north of Tullah (Fig. 1.1) in the southeast corner of the study area. Access is gained to the area via the Bulgobac Falls Track, which runs north from Boco Road just west of the Murchison Highway. The track terminates in the south of the study area, giving access to outcrop along the Bulgobac and Que rivers and the Emu Bay Railway. Mapping was restricted to these areas, the tracks and three east-west grid lines cut at 200 metre intervals north from 5391800 mN AMG. The topography of the area is dominated by a northeast-southwest trending ridge up to 560m above mean sea level, which drops steeply to 300m into the Que River to the south and east. Vegetation within the area is mainly dense rainforest with occasional areas of more open eucalypt forest.

1.3 Regional Geology

1.3.1 Introduction to the Mount Read Volcanics

The rocks within the Bulgobac Falls area are part of the Middle to Late Cambrian Mount Read Volcanics. This belt of diverse lavas intrusives and volcaniclastic rocks (McPhie and Allen, 1992) stretches for 200km through western Tasmania between Elliott Bay and Deloraine (Fig. 1.2) and constitutes the eastern side of the Dundas Trough (Corbett, 1992). The Dundas Trough was a Cambrian depositional basin lying between the Precambrian Tyennan and Rocky Cape regions. The presence of trilobites, turbidites, hyaloclastite

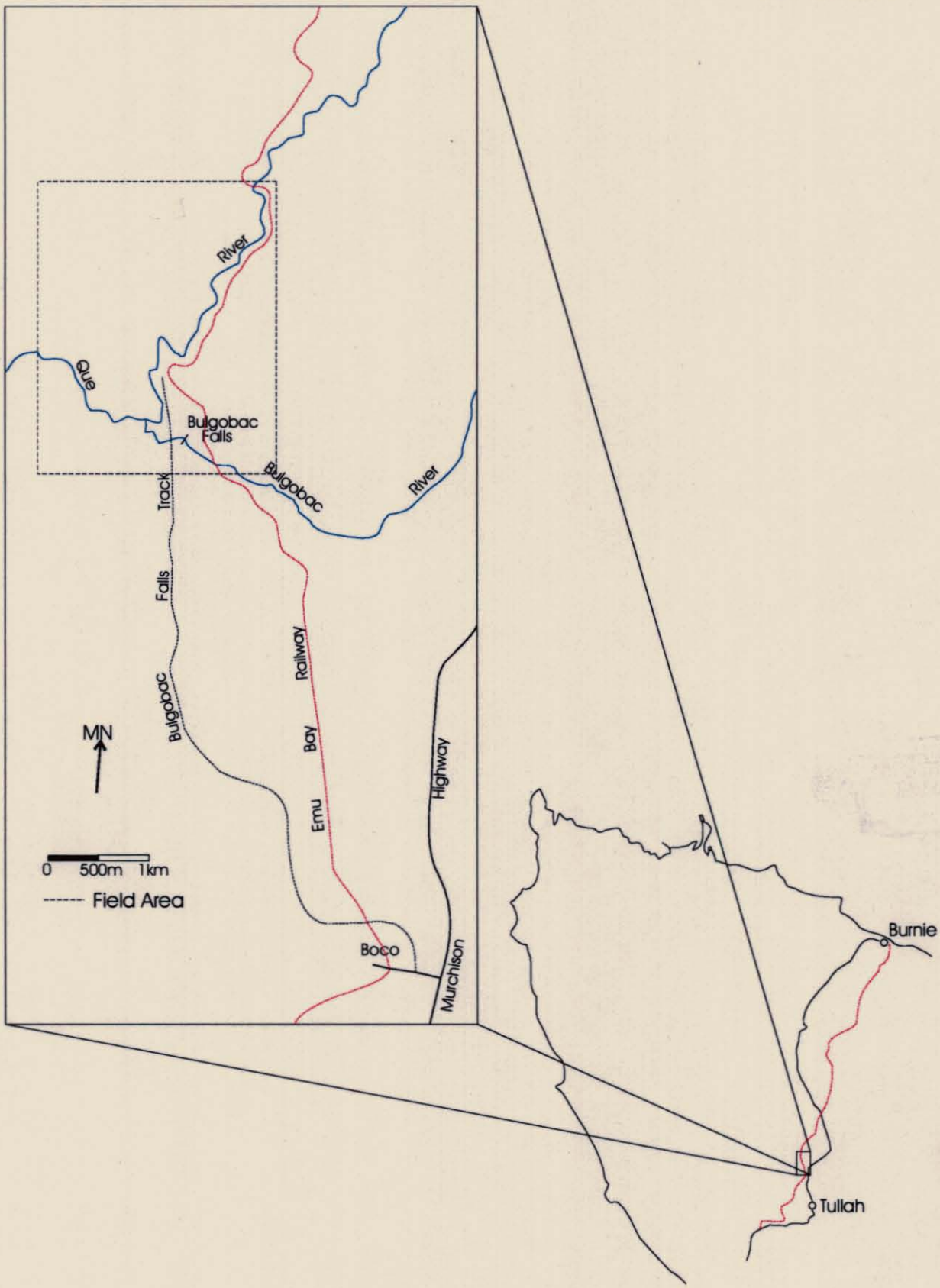

Figure 1.1: Location of the Bulgobac Falls and the field area.

5 cm

breccias, pillow basalts and massive sulphide mineralisation indicates the Mount Read Volcanics were mainly deposited in a submarine environment, below storm wave base (McPhie and Allen, 1992).

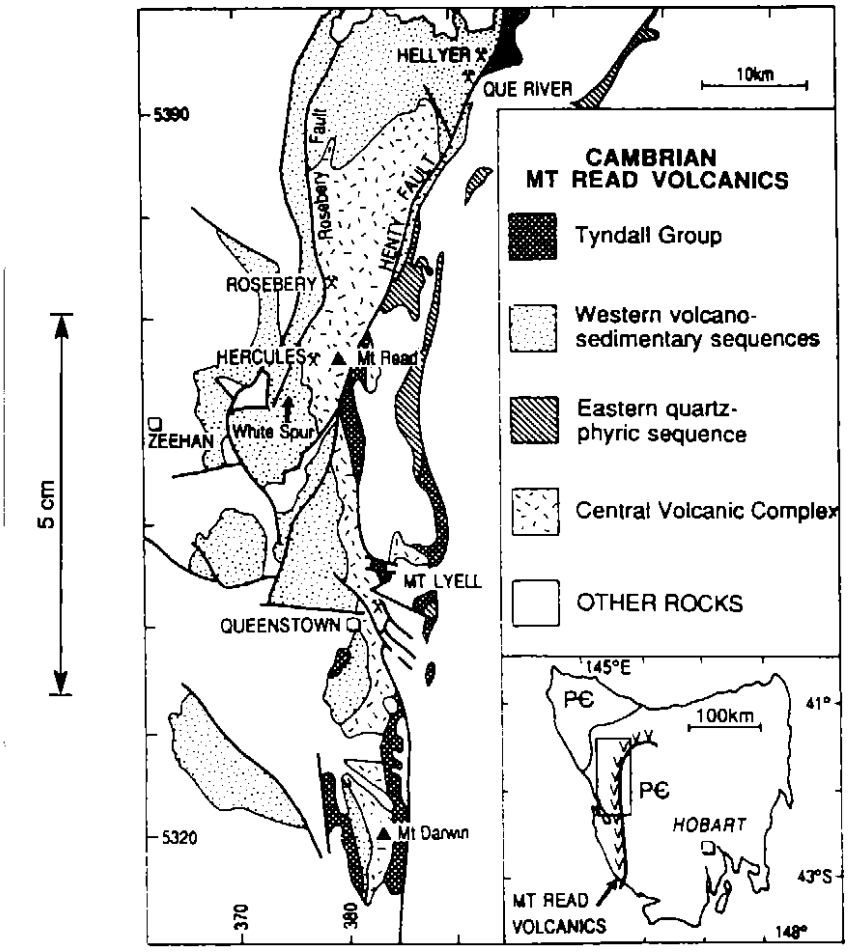

Figure 1.2: Mount Read Volcanics showing distribution of major lithostratigraphic units (McPhie and Allen, 1992).

Most of the Mount Read Volcanics rocks have been subject to considerable deformation and have been moderately to highly altered. The original textures and compositions have been variably modified making original facies relationships difficult to determine (Corbett, 1992). Further complication arises from the prominent NNE trending Henty Fault, which bisects the belt longitudinally and disrupts the stratigraphy.

The Mount Read Volcanics can be broadly divided into five main lithostratigraphic units (Corbett, 1992): The Sticht Range Beds, the Central Volcanic Complex (CVC), eastern quartz phyric sequence, western volcano-sedimentary sequences and the Tyndall Group.

Their stratigraphic relationships are inferred in Figure 1.3. The geology of the Bulgobac Falls area is within the western volcano-sedimentary sequences.

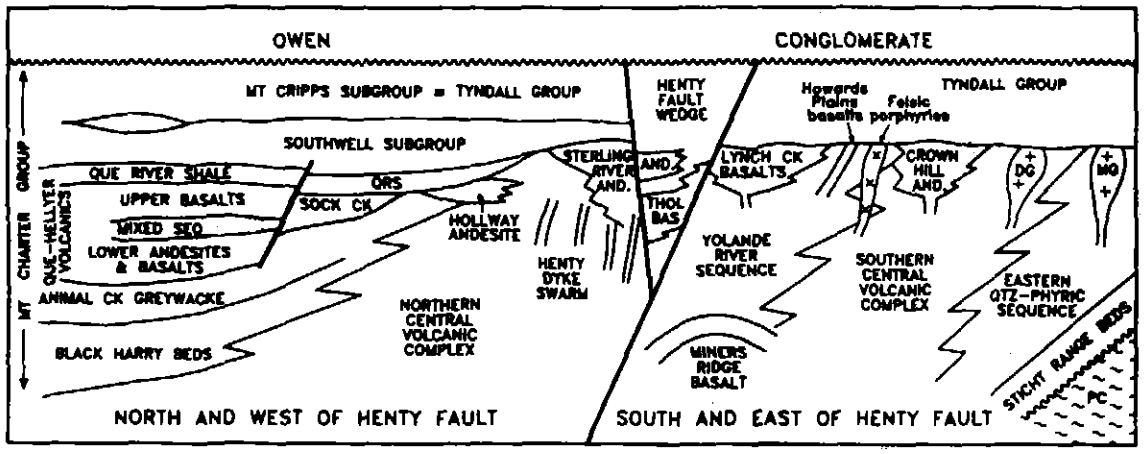

Figure 1.3: Schematic diagram showing inferred relationships of major lithostratigraphic and lithological units of the Mount Read Volcanics. DG = Darwin Granite, MG = Murchison Granite (adapted from Corbett, 1992).

The Sticht Range Beds

The Sticht Range Beds are a thin layer of siliciclastic conglomerate, sandstone and minor siltstone that lies unconformably on Precambrian basement along the eastern margin of the Mount Read Volcanics (Corbett, 1992). Baille (1989) suggested the sequence shows a progression from a fluvial environment, to a shallow marine environment and the to a deep marine environment.

Eastern Quartz Phyric Sequence

This sequence overlies the Sticht Range Beds along the eastern side of the Mount Read Volcanics. It comprises quartzofeldspathic lavas, syn-volcanic intrusions and volcaniclastic rocks (Corbett, 1992; White, 1996). Deposition in a subaqueous environment is inferred from bedded sandstone, siltstone and mudstone within the sequence (McNeill and Corbett, 1992; Corbett, 1992).

Central Volcanic Complex

The Central Volcanic Complex occupies the central portion of the Mount Read Volcanics and is separated into two parts by the Henty Fault (Fig. 1.2). Corbett (1992) describes the sequence as mainly feldspar-phyric and dacitic lavas, pumiceous volcaniclastics and massive dome shaped lavas. South of the Henty fault, the complex is intruded by granites and potassic lavas. These are not found in the northern portion of the CVC.

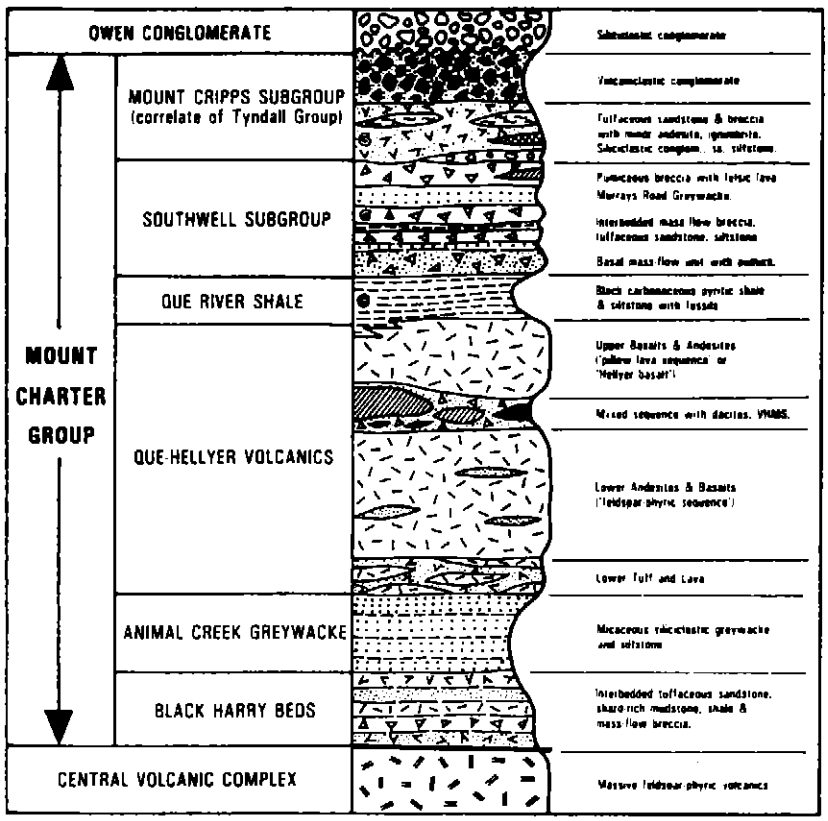

Figure 1.4: Stratigraphic column and terminology for the Mount Charter Group in the Hellyer-Que River area. (from Corbett, 1992)

Western Volcano-sedimentary Sequences

To the north and west, the Mount Read Volcanics are flanked by sequences of interbedded mass-flow deposits, turbiditic sandstones, laminated mudstones, micaceous siltstones and black shales that comprise the Western volcano-sedimentary sequences (Corbett, 1992). These are interpreted as having been deposited in a submarine setting, below storm wave base, based on the bed forms, the fossils present, pillow basalt lavas and the associations between hyaloclastite breccias and rhyolitic, basaltic and andesitic lavas (McPhie and

Allen, 1992). Corbett (1992) divides the sequences into four major units, largely focussed around the Henty Fault. The Henty Fault Wedge occurs between the North and South Henty Faults, the Yolande River Sequence is found south of the Henty Faults and the Dundas Group is to the north of the faults. The fourth unit is the Mount Charter Group which is found in the Pinnacles – Sock Creek – Mt. Charter – Mt Cripps area (Corbett, 1992; McKibben, 1993). The stratigraphy of the Mount Charter Group is outlined in Figure 1.4. Of particular interest for this thesis is the Mount Cripps Subgroup, the uppermost unit, which is the name given by Corbett (1992) to correlates of the Tyndall Group within the Mount Charter Group.

The Tyndall Group

The Tyndall Group is a belt of predominantly mass-flow sandstones and breccias overlain by abundant volcaniclastic conglomerates, that outcrops discontinuously south of the Henty Fault (Corbett, 1992; White, 1996). It is the youngest sequence of the Mount Read Volcanics, overlying the CVC, the eastern quartz-phyric sequence and the Yolande River Sequence. In the north, correlates of the Tyndall Group are at the top of the Mount Charter Group, and in both areas the Tyndall Group and its correlate are overlain by the Owen Conglomerate (Corbett, 1992). White (1996) and White and McPhie (1996) have defined the stratigraphy of the Tyndall Group (Fig. 1.5). The Zig Zag Hill Formation is dominated by polymict volcaniclastic conglomerates and sandstones, with minor laminated mudstone and rhyolite (White, 1996). The Comstock Formation will be discussed in detail in chapter 4. Corbett (1992) and White (1996) suggest a subaqueous depositional environment adjacent to a subaerial to shallow marine volcanic terrain.

1.3.2 Tectonic Setting

The tectonic setting for the emplacement of the Mount Read Volcanics has been the subject of much conjecture. Various models have been proposed, which have been reviewed by Corbett and Turner (1989). Corbett *et al* (1972), proposed an extensional plate boundary forming an intracontinental rift. Both east dipping and west dipping subduction zones at convergent plate boundaries have also been proposed (Corbett and Lees, 1987; Corbett and Turner, 1989). Berry and Crawford (1988) and Crawford and Berry (1992) put forward a model based on comparisons with modern day settings that have produced similar distinctive lavas to those found in the Mount Read Volcanics. This

model involves the collision between a passive continental margin and a forearc.

1.3.3 Deformation and Metamorphism

Two major periods of deformation are evident for the Mount Read Volcanics, a Late Cambrian and a Middle Devonian (Williams, 1989). The Cambrian event is mainly fault related and is responsible for the Henty Fault, which significantly disrupts the stratigraphy of the Mount Read Volcanics. The Rosebery Fault also became active during this time (Corbett, 1992). The Cambrian event has similar structural trends to the Devonian event although the Cambrian event has only locally developed cleavages that are largely overprinted by the Devonian event (Corbett and Lees, 1987). The Darwin and Murchison Granites (Fig. 1.3) were emplaced by an intrusive event in the Late Cambrian that resulted in K feldspar/magnetite alteration (Polya *et al*, 1986). Andesitic-basaltic magmas and quartz-feldspar porphyries were also intruded during this period (Pemberton and Corbett, 1992).

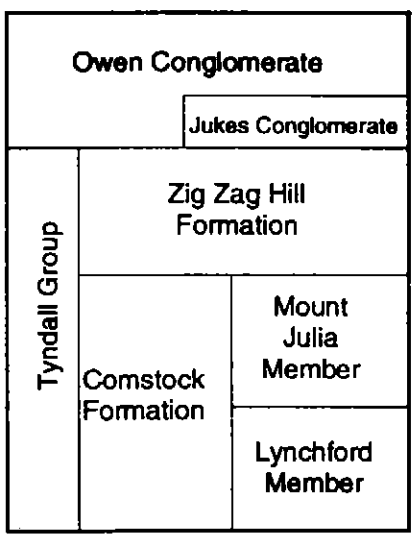

Figure 1.5: Tyndall Group stratigraphic scheme(White, 1996)

The Devonian event can be correlated to the Tabberabberan Orogeny and has been related to four deformation phases, outlined in chapter 3 (Table 3.1) (Seymour, 1980; Seymour and Calver, 1995). In the northern Mount Read Volcanics, prehenite-pumpellyite facies metamorphism is thought to have developed during this event. In the south, the development of lower greenschist facies metamorphism is related to the Devonian

deformation (Offler and Whitford, 1992 and Eastoe *et al*, 1987 in White, 1996).

1.4 Previous Work

The area covered by this thesis has a brief exploration history. It has been included within exploration leases since the early sixties, however detailed exploration work has mostly been done on parts of those leases to the south and west of the Bulgobac Falls. Rio Tinto geologists mapped within the area as part of a regional mapping program and suggested that the contact between Dundas Group rocks and underlying porphyries in the Bulgobac Falls area represented an angular unconformity (Campana *et al*, 1960). Banks and Solomon (1961) disputed this, arguing that there was a disconformity at this point but no evidence for an angular unconformity.

From 1963 Comstaff Pty. Ltd. focused on the area from Boco Siding through to the Silver Falls prospect southwest of the field area, as a result of stream sediment sampling, and conducted reconnaissance soil geochemistry. EZ Co., with various partners, held the lease encompassing the area from 1972 to 1987, focussing most of their exploration on mapping and geochemical analysis of base metal anomalies to the northwest and southwest of the area (Green, 1995).

Pasminco Exploration operated the lease from 1990 until they relinquished the portion that includes the Bulgobac Falls area in 1995. They mapped extensively as part of a regional mapping program and correlated the local geology to the upper part of the Mount Charter group (Poltock, 1993). A regional aeromagnetic survey was also conducted at this time which showed a change in the magnetic character of the rocks within the Bulgobac Falls area (Kirsner 1992).

Collins (1980) compiled a 1:36680 map that incorporated the area for the Tasmania Department of Mines. This was accompanied by an explanatory report prepared by Collins *et al* (1981). The more recent production of the 1:25000 'Charter' sheet is largely based on the older map (Corbett *et al*, 1995).

During the 1980's the Hydro Electric Commission also mapped the outcrop within the area as part of a survey for proposed dams along the Que River. The geology of the area was

correlated to the contemporary Dundas Group sequence (Wilson, 1989). They also conducted an extensive program of shallow drilling along the river bank and the Emu Bay Railway, however much of the drill core has since been destroyed.

McKibben (1993) mapped in the Pinnacles area approximately 5 km south of the Bulgobac Falls area. This region included a finger-like projection of intrusive rhyolite surrounded by sandstones, siltstones and greywackes which were equated to Southwell Subgroup and Mount Cripps Subgroup.

1.6 Aims and Method

The principle aims of this thesis are:

1) To map the structure of the area to the northwest and west of the Bulgobac Falls and to test the structural models of previous workers.
2) To produce a detailed description of the stratigraphy to the above of a large porphyry in the Bulgobac Falls area.
3) To correlate this stratigraphic sequence with the Tyndall Group and its correlates elsewhere in the Mount Read Volcanics.
4) To recognise the base of the Tyndall Group correlate in the Bulgobac Falls area.
5) To compare the aeromagnetic data for the area with the magnetic susceptibility of the rocks and determine the reason for magnetic variations within the rocks.

To achieve these aims, data on the field area was collected by mapping and sampling outcrop during March 1997. The magnetic susceptibility of the outcrop was also measured during this time. Samples were subject to petrographic analysis to determine the mineral composition of the rocks and their variation through the stratigraphic sequence. This sequence was then compared with Tyndall Group stratigraphy. Geochemical analysis, including XRF analysis and isotopic analysis of carbonate units, was conducted to enable correlation of the rock units both within the stratigraphy of the area and with similar stratigraphic sequences elsewhere. Heavy mineral separation was carried out to enable comparison of highly magnetic rock units with those that had a low magnetic signature, to determine if the different magnetic character was the result of differences in source material or the result of alteration.

Chapter 2: Stratigraphy and Sedimentology

2.1 Introduction

This chapter examines the stratigraphy of the Bulgobac Falls area and the sedimentological processes involved in deposition of the sequence. Figure 2.1 is a stratigraphic column prepared from measurements taken along the Bulgobac and Que rivers, with some adjustment due to this not providing a straight line perpendicular to the stratigraphy and variations in bedding thicknesses along strike. The approximate line represented by this column is indicated in Figure 2.2.

2.1.1 Terminology

Lithofacies: A mappable subdivision of the overall stratigraphy, which can be differentiated from the rest of the stratigraphy based on lithology or sedimentary processes.

Unit: A mappable subdivision within a lithofacies.

Volcaniclastic: A non-genetic term for a rock with a clastic fabric resulting from volcanic processes.

Calcareous: A rock with >50% calcium carbonate.

Rhyolite: Volcanic rock with abundant quartz and common feldspar phenocrysts in a highly siliceous groundmass.

Andesite: A volcanic rock with no visible quartz, abundant plagioclase and common clinopyroxene phenocrysts in a groundmass of plagioclase microlites and granular pyroxene.

Basalt: A volcanic rock with abundant mafic and common plagioclase phenocrysts in a groundmass of plagioclase microlites and granular pyroxene.

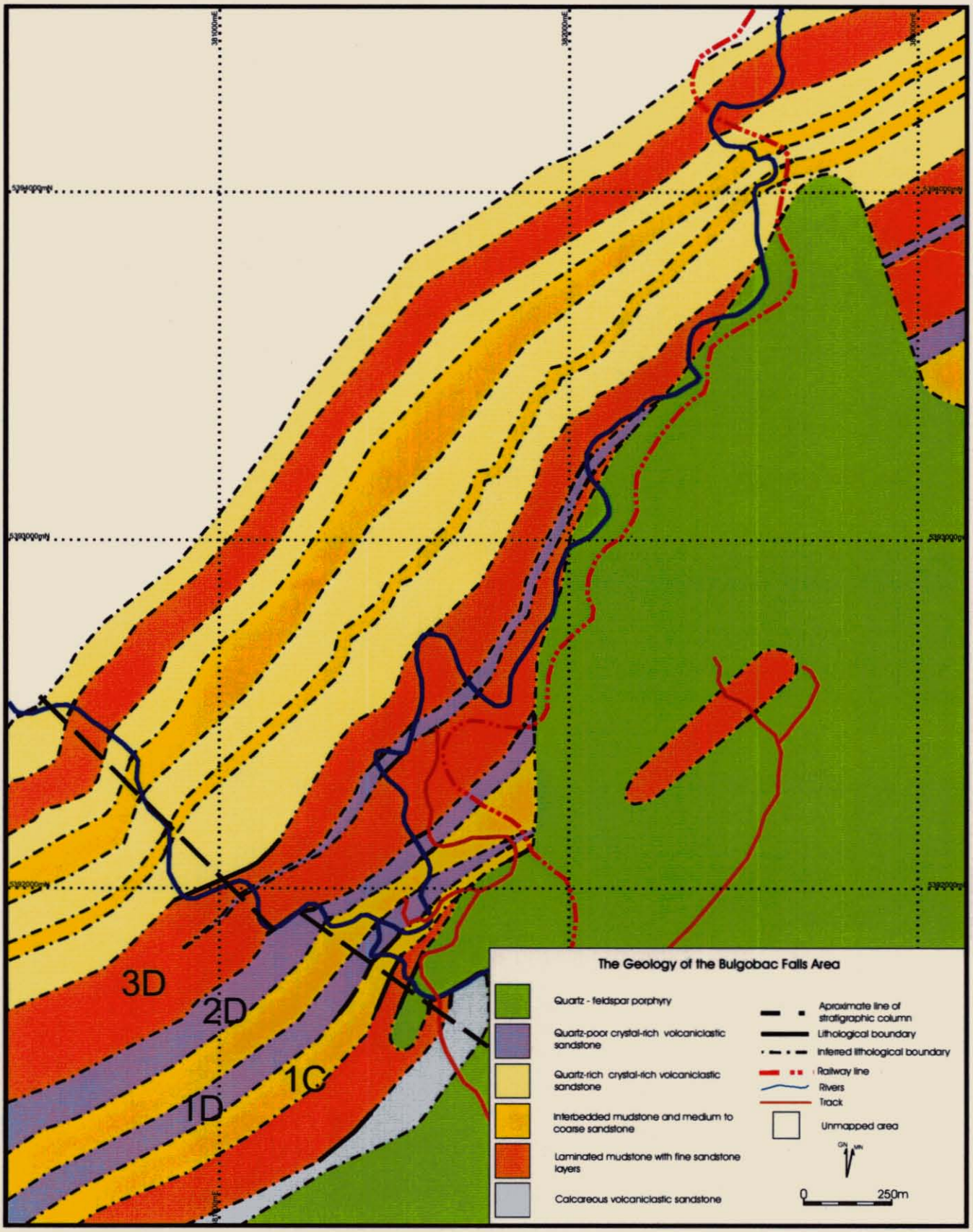

Figure 2.1: Lithological map of the Bulgobac Falls area showing approximate line of stratigraphic column and identifying individual units mentioned in text.

5 cm

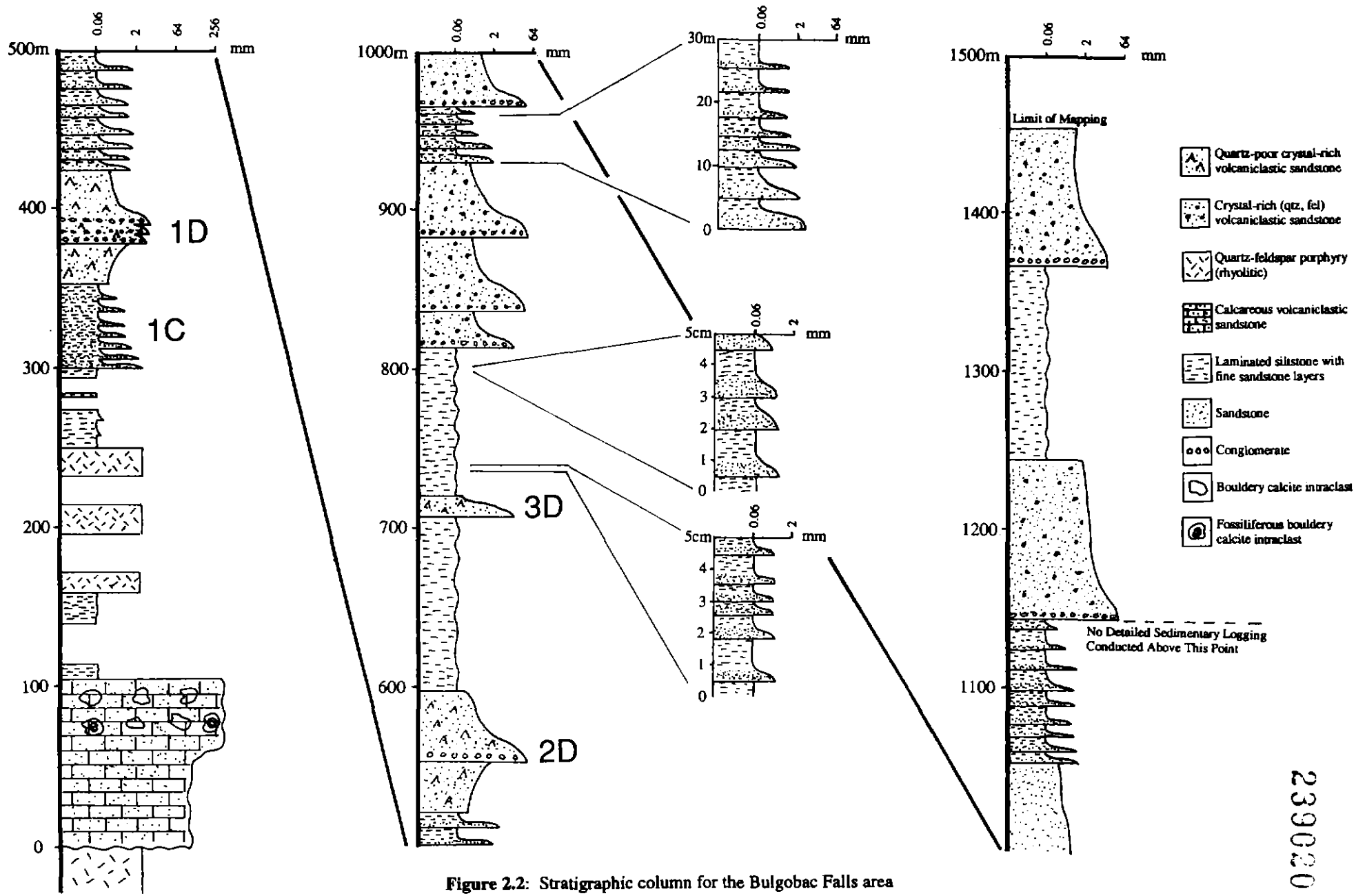

Figure 2.2: Stratigraphic column for the Bulgobac Falls area

Variations between units of the same lithofacies will be discussed at the end of each description where they are considered significant. The units are labelled in Figure 2.2 and the stratigraphic column (Fig. 2.1) according to their lithofacies and there stratigraphic relationship to each other ie. unit 1B is the oldest unit of lithofacies B, 2B the next youngest and so on. This has only been applied where variations have been described. Facing direction within the field area was determined from the fining upwards sequences particularly evident within the mass flow units. These all fine in a westerly direction indicating the sequence youngs in this direction.

2.2 Lithofacies

2.2.1 Facies A:

Calcareous Volcaniclastic Sandstone

The calcareous sandstone is the basal sedimentary unit in the Bulgobac Falls area. This unit contains abundant sub-rounded limestone clasts up to .5 metres in diameter in its upper 40 metres (>80%). The limestone clasts are either sparry or micritic calcite (Fig. 2.4a.) with some of the micritic clasts having sparry calcite veins woven through them. The limestone is generally creamy white, while the sparry calcite veins are pale to dark grey. The sparry calcite veins were mauve when stained with Alizarin Red S and potassium ferricyanide, indicating they are enriched in iron (Adams *et al, 1994).* Isolated clasts contain abundant fossils, including trilobites (Fig. 2.3a.) and ostracods (Fig. 2.3b). One of the trilobite fauna has been tentatively identified as a dolichometopid trilobite of the genus *Amphoton*, dating the original limestone source as Middle Cambrian (J. Jago pers. comm.).

The limestone clasts are contained above and within a medium to coarse grained volcaniclastic sandstone. The sandstone is poorly sorted, pale yellow to grey, crystal-rich (40-80%) and grain supported with generally angular to sub-angular and occasional sub-rounded clasts. A volcanic source for the sediments is indicated by the presence of rounded, embayed quartz crystals, sanidine lathes and lathe fragments and minor rhyolitic lithic clasts (<5%). Feldspar crystals have been extensively altered to sericite throughout

the facies.

Below the bouldery upper layer, the unit is interbedded, with layers in which there is a greater percentage of matrix to clasts. Some layers have up to 30% matrix, while one layer was seen to have as little as 5%. The matrix in all cases appears quartzofeldspathic and contains chlorite and carbonate.

2.2.2 Facies B:

Laminated Micaceous Mudstone and Fine Sandstone

The laminated mudstone and fine sandstones (Fig. 2.4g) occur throughout the field area. Considerable variation in colour was be seen, with the most common being dark grey-green and pale grey, but also dark grey, creamy grey and yellow-green. The mudstones in particular frequently have a micaceous sheen and muscovite is pervasive in thin section as is chlorite. There are both graded systems where the fine sandstones with sharp basal contacts fine upwards to mudstones, and distinct layers with sharp upper and lower contacts. Quartz is common (15-20%) throughout the coarser layers and is generally sub-angular to sub-rounded. Bedding is parallel, laterally extensive and generally thin (3-15cm), and with the exception of the fining upward sequences, no sedimentary structures were observed. The fine sandstones occasionally occur as massive beds, up to 1.5m wide, but are more frequently thin layers of less then 1cm within the mudstone.

An outcrop of mudstone within the porphyry is considered to be a continuation of the oldest bed within, however it should be noted that this correlation is based solely on the outcrop occurring along strike from the contiguous sedimentary sequences and a similarity in bedding orientation. Outcrop of the isolated mudstone was poor and highly weathered making a compositional correlation impossible.

2.2.3 Facies C:

Interbedded Mudstone and Medium to Coarse Sandstone

This facies occurs throughout the stratigraphy of the area. Thin beds of sandstone and mudstone dominate, with sandstone beds never exceeding 1.5m thick. The sandstone beds have sharp basal contacts and fine upwards to mudstones. Mudstone beds become increasingly dominant upwards within each unit of the facies and the sandstone beds thin

and fine.

Variations

Unit 1C

Just below the upper contact with the overlying volcaniclastic sandstone along the Que River is a finely laminated dark grey mudstone with considerable framboidal pyrite (10%) and minor idiomorphic pyrite grains (Fig. 2.4h).

2.2.4 Facies D:

Quartz-Poor Crystal-Rich Volcaniclastic Sandstone

The quartz-poor crystal-rich volcaniclastic sandstone is distinguished by the lack of quartz crystals (<10%) and a relative abundance of clinopyroxene (>15%) and feldspar (>30%) (Fig. 2.4c). Lithic clasts are common (15-20%), usually andesitic to basaltic porphyries but angular to sub-angular crystals are dominant (>50%). Occasional sub-angular quartz-rich schists with strong mica foliations are also seen, as are rounded chert grains. Where seen, quartz crystals are angular to rounded, with the rounded crystals tending to be embayed suggesting a volcanic origin, and may show undulose or straight extinction. Fractured grains with jigsaw fit patterns suggesting in-situ brecciation are also found. Feldspar crystals are mostly sanidine or plagioclase and show significant alteration to sericite. The matrix is dominated by chlorite, in most cases Fe-rich, indicated by deep violet birefringence (Fig. 2.4e) (Deer *et al,* 1992). In hand specimen, this facies generally has a dark green-grey appearance.

Variations

Unit 1D

The initial bed is a medium grained, pale grey-green sandstone which coarsens upwards to a course sandstone. Dark grey mudstone intraclasts were found locally at the base of this bed. Repeated fining upward sequences then occur, with conglomerate bases containing 3cm rounded lithic clasts and sharp basal contacts. The uppermost bed is the dominant bed within this sequence. The rock is a creamy white and pale green-grey in contrast with later units in this facies. The clasts are contained in a chloritic matrix which is distinct from later beds in this facies by not being iron-rich.

Figure 2.3: Photomicrographs of fossils from calcareous volcaniclastic sandstone

A)Trilobite, showing characteristic hook shape, in clast of sparry and micritic calcite.. Sample J2, plane polarised light.

B) Ostracod in of sparry calcite. Sample J2, plane polarised light

A

B

Figure 2.4: Photomicrographs of principle lithofacies of Bulgobac Falls sequence

a) Calcareous volcaniclastic sandstone showing sparry calcite clasts (left) and micritic calcite clasts (right) in a sandy matrix with quartz and sericite altered feldspar. Sample P73, crossed nicols.

b) Embayed quartz crystal showing some evidence of recrystallization. From quartz feldspar porphyry, sample P14, crossed nicols.

c) Quartz-poor crystal-rich volcaniclastic sandstone showing abundant sericite altered feldspar (fld) and clinopyroxene (cpx) and minor quartz(q). Sample P54, crossed nicols.

d) Quartz-poor crystal-rich volcaniclastic sandstone showing abundant sericite altered feldspar (fld) and magnetite (m) and minor quartz in a chloritic matrix. Sample L9, plane polarised light.

e) Fe-rich chlorite(cl) in a quartz-poor crystal-rich sandstone with abundant altered feldspar (fld), minor quartz (q) and a metamorphic quartzite grain (mqtz). Sample P35, crossed nicols

f) Quartz-rich crystal-rich volcaniclastic sandstone showing large rounded lithic porphyritic andesite (L), minor chlorite (cl) and metamorphic quartzite grain (mqtz). Sample P44, crossed nicols

g) Laminated fine sandstone showing fining upward trend. Sample P52, plane polarised light

h) Laminated mudstone with framboidal and euhedral pyrite. Sample P29.

239026

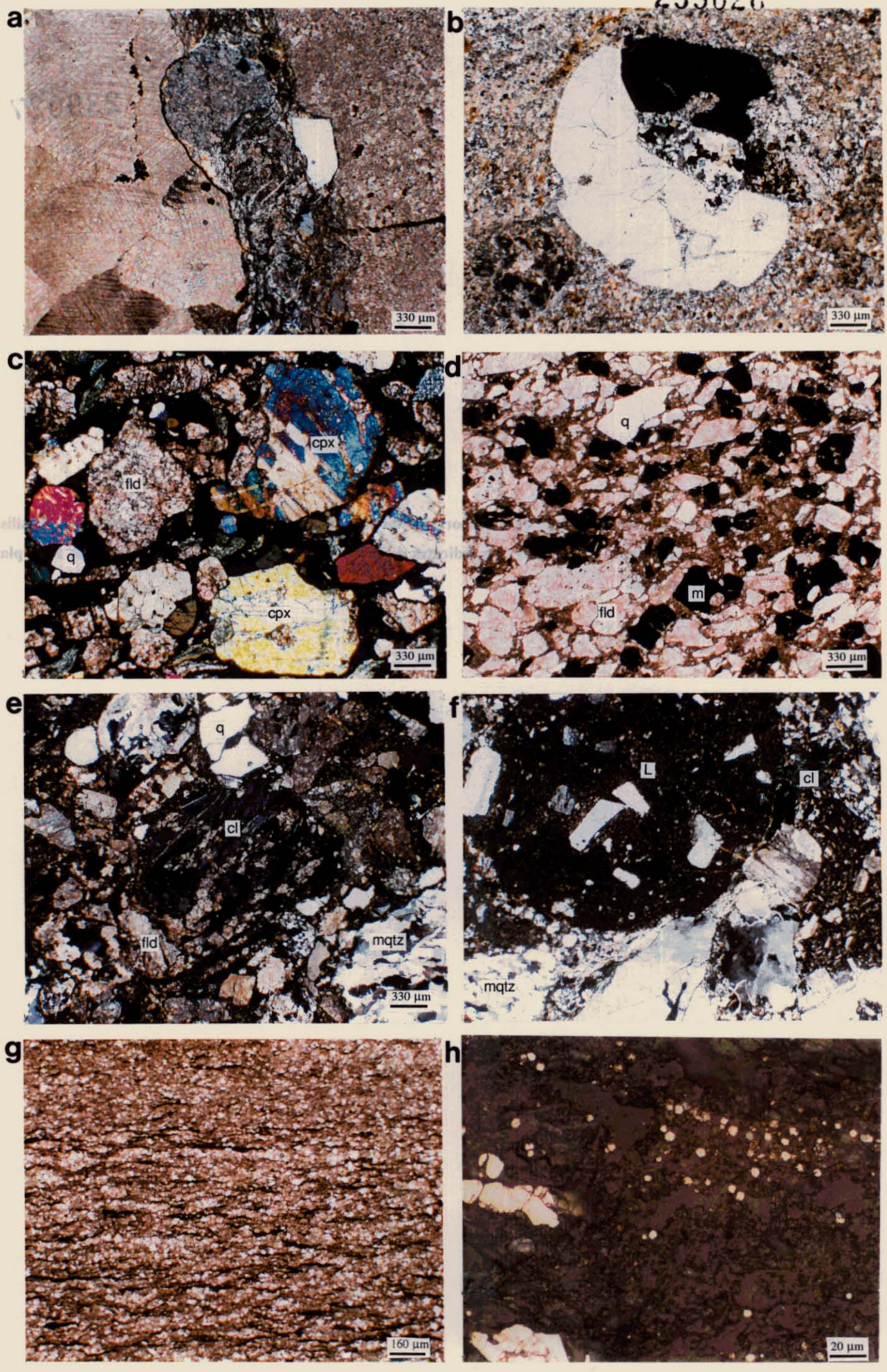
a
330 µm
b
330 µm
c
cpx
fld
q
cpx
330 µm
d
q
m
fld
330 µm
e
q
cl
fld
mqtz
330 µm
f
L
cl
mqtz
g
160 µm
h
20 µm

Figure 2.5: Clast from quartz-poor crystal-rich volcaniclastic sandstone containing fossilised calcareous algae. Lower diagram indicates differing types of algae within clast. Sample P35, plane polarised light.

239028

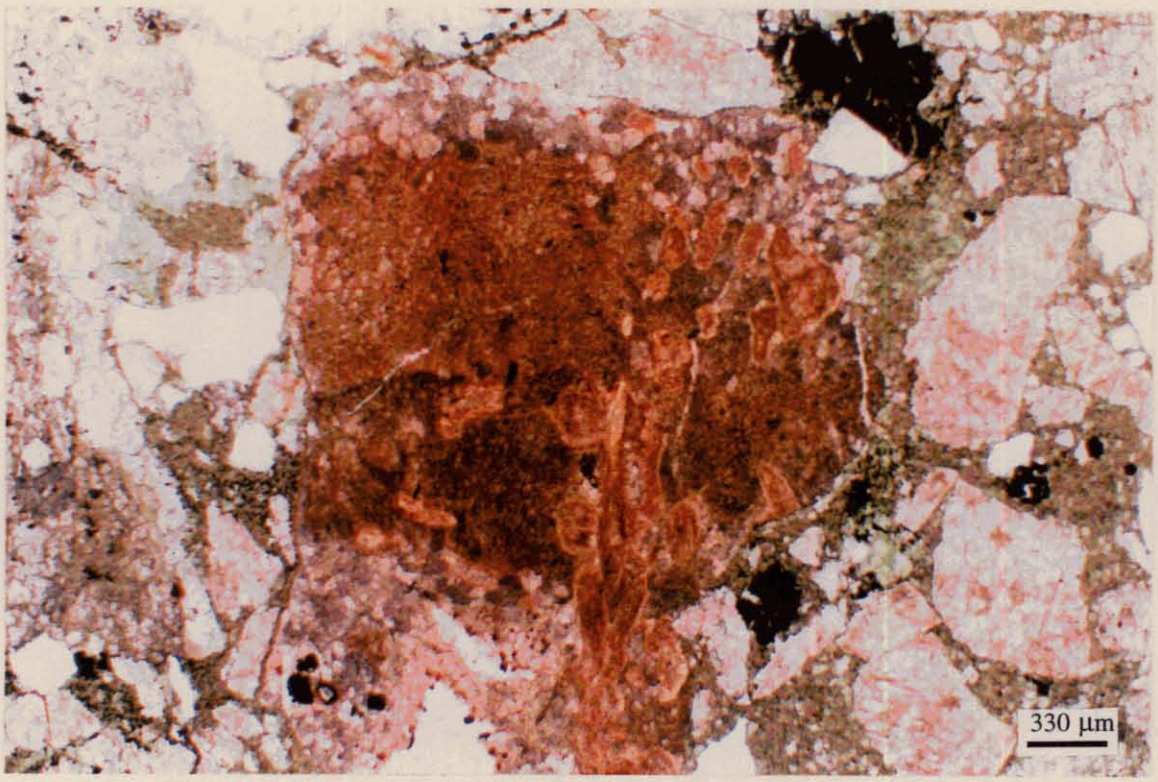

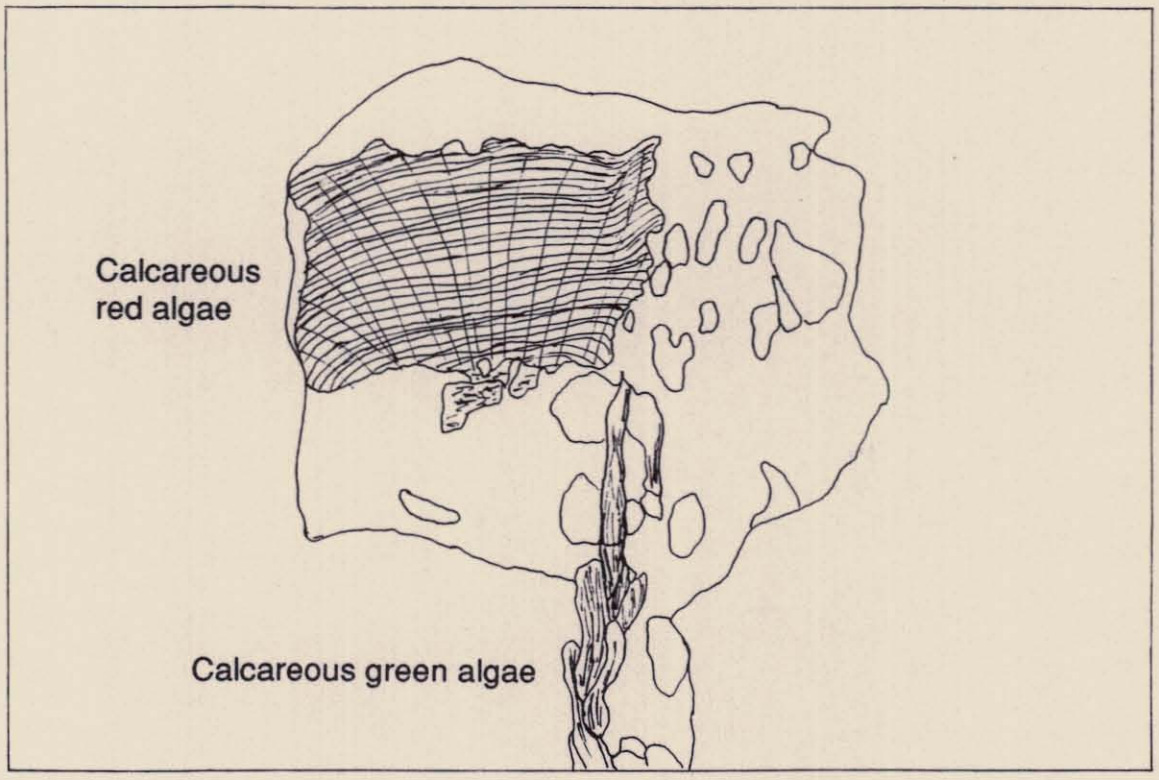

Unit 2D:

The next quartz-poor crystal-rich facies begins with a medium grained, moderately sorted, dark grey sandstone (Fig. 2.4d) which is distinctive because of its high magnetic signature ($2600x10^{-5}$nT). No lithic clasts were seen in this bed, with sericite altered plagioclase and sanidine crystals dominating (40%). Opaque minerals are also abundant, with magnetite comprising 20% of the rock and hematite approximately 10%. Euhedral pyrite grains, a few with goethite rims, form veins through the bed and constitute about 5% of the overall composition. This bed also contains traces of chalcopyrite and muscovite and coarsens upwards. A normally graded bed overlies this, with little overall variation in texture. Further north along strike however, the unit coarsens, with lithic clasts up to 5mm at the base of the bed.

Unit 3D

Along the southern intersection of this unit with the Que River, the sandstone is well sorted and a single, thin bed. At it's next two intersections of the river to the north, this bed thickens, becoming coarser, poorly sorted and has a conglomeratic base. In this region, the bed is texturally similar to earlier beds of this facies, with abundant clinopyroxene, feldspar and lithic clasts of volcanic and metamorphic origin. At the point of its northernmost crossing of the Que River, this bed has thinned again and become a medium to coarse, moderately sorted sandstone. The lensing of this bed is interpreted as being a result of the bed being deposited in a single mass flow event that has been channeled, possibly by topography, or has been a small localised event. As a result, the thin, finer grained section to the south represents an edge of the flow, where only finer material has been deposited in later and more dispersed settling from the main flow. The northern intersection is given a similar interpretation, however the bed has not thinned as significantly and so may not lens out as rapidly.

Within this bed there are also fossiliferous clasts containing calcareous algae (Fig. 2.5). Although precise identification of these algae is difficult and not within the scope of this thesis, at least two different forms appear to be contained within the observed clast. The net-like structure in the upper potion of the clast is most similar to calcareous red algae, possibly of the genus *Solenpora,* while the central stem-like is possibly the calcareous

green algae, genus *Palaeoporella* (Wray, 1977).

2.2.5 Facies E:

Quartz-Rich Crystal-Rich Volcaniclastic Sandstone

Two factors separate this facies from facies D. First, this facies contains significantly more quartz (>20%) and second, clinopyroxene grains are rare (Fig. 2.4f). Beds generally fine upwards, and have a conglomeratic base, with rounded lithic clasts up to 3cm across. The sandstones are grain supported with angular to sub-angular grains in a chlorite-rich quartzofeldspathic matrix, although some igneous lithic clasts and quartz grains are sub-rounded to rounded. Lithic clasts are more common (25%) than in facies D and include porphyritic andesites and basalts, minor mafic lavas, quartz-rich schists and sandstones and chert clasts. Feldspar crystals predominate (30%), with both sanidine and plagioclase present, although there appears to be some reduction of the feldspar in the upper-most beds and a corresponding increase in quartz content. The feldspar crystals show some evidence of sericite alteration. The units within this facies have been correlated along strike based on their relative positions within the sequence and there increased quartz content.

2.2.6 Facies F:

Quartz-Feldspar Porphyry

The quartz-feldspar porphyry is a creamy white to pale green or pink quartz and feldspar-phyric rock. Phenocrysts of quartz and feldspar may be up to 4mm in width. Quartz phenocrysts are typically embayed, rounded to sub-rounded and have melt inclusions (Fig. 2.4b). Occasionally they also show evidence of recrystallisation around their rims. Feldspar phenocrysts are either sanidine or plagioclase, with plagioclase slightly dominant. The phenocrysts are frequently euhedral, but some subhedral to anhedral grains are observed and all show varying degrees of sericite and chlorite alteration. The matrix is quartzofeldspathic, with partial alteration to sericite and chlorite. It contains a trace of fine grained muscovite.

Most of the eastern margin of the field area is dominated by the quartz-feldspar porphyry. Previously it has been described as part of a major body of porphyry intruding the Mt. Charter Group west of the Murchison Highway (Corbett and Komyshan, 1989). Within the Bulgobac Falls area this unit is clearly intrusive as it can be seen to truncate the

sedimentary units at its western margin and must therefore post-date deposition of at least part of the sedimentary sequence described here. No indication of a peperitic margin to suggest shallow intrusion into unconsolidated sediments (Williams and McBirney, 1979) or of contact metamorphism was seen. The tongue of porphyry that intrudes upwards stratigraphically near the Bulgobac Falls and the possible distortion seen in the bedding on the north-western side of this may indicate the porphyry was intruded as a syn-volcanic sill (McPhie *et al*, 1993). The high ratio of quartz to feldspar and of sanidine to plagioclase together with the low level of ferromagnesian minerals classifies this rock as a rhyolitic intrusive (McPhie *et al*, 1993; Compton, 1985).

2.3 Sedimentary Processes

The Western volcano-sedimentary sequences are marine deposited sequences which include mass-flow deposits, turbiditic sandstones and micaceous mudstones amongst other lithologies (Corbett, 1992). Turbidity currents are one type of mass-flow, and most closely correlate with the type of process which has formed the sequence in the Bulgobac Falls area.

Turbidity currents are particle flows in which the particles are suspended by the turbulence of the interstitial fluids (McPhie *et al*, 1993). Normally graded, or upward fining, bedding is characteristic of turbidity currents (Kuenen and Migliorini, 1950). Low-density turbidity currents are relatively slow moving currents which support finer grained materials, up to medium sand-size (Lowe, 1982). As the flow decelerates, it deposits the suspended material, with the heavier, coarser material settling first, forming graded beds. Further deceleration gradually changes the depositional processes and results in a typical Bouma sequence (Fig. 2.6a) (McPhie *et al*, 1993). High-density turbidity flows are more energetic, carrying larger particles at greater speeds and over longer distances than low-density currents. The resulting beds are thicker (metre scale) than the low-density flow beds which are centimetres to tens of centimetres thick (McPhie *et al*, 1993). In an idealised setting, they may be characterised by an initial reverse graded bed, which is succeeded by a normally graded bed (Fig. 2.6b) (Cas and Wright, 1987; McPhie *et al*, 1993).

The volcaniclastic sandstones of facies D and E are interpreted as being deposited by high-

density turbidity currents based on their clast size, normal grading and bed thickness. Within facies D, there are also two sequences of reverse graded beds underlying normally graded beds. Although these beds appear to have a sharp contact between the reverse and normally graded beds rather than a gradual change through a non-graded stage, this still supports turbiditic deposition. The variation may represent the difference between the idealised models and real depositional environments. It is possible these represent separate depositional events, with the second normally graded event removing the upper portion of the original bed with a reversely graded base.

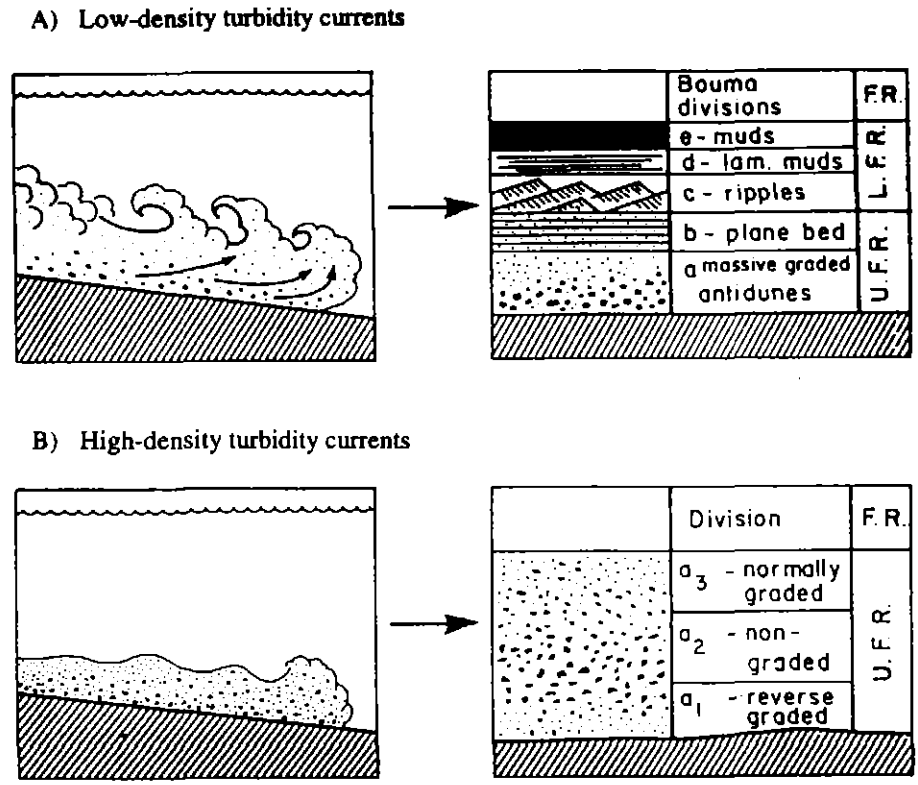

Figure 2.6: Characteristics of low and high density turbidity currents and their deposits. U.F.R. = upper flow regime, L.F.R. = lower flow regime (from Cas and Wright, 1987).

The laminated mudstone with fine sandstone layers (facies B) is most likely the result of low-density turbidity currents, indicated by the normal grading in the fine sandstone layers. The mudstone layers will also include normal background pelagic sedimentation typical of a marine environment. A similar interpretation is made for the interbedded mudstone and medium to course sandstone (facies C), except that the current density would have been greater than that for facies B.

Aside from the absence of bouldery clasts within the lower half of facies A and their

predominance within the upper half, the calcareous sandstone is poorly sorted overall. It does not show evidence of grading which would support it being deposited by turbidity currents. The texture of the bed overall suggests a grain flow or debris flow as the method of deposition. Grain flows are down-slope movements of grains independent of interstitial fluid and are characteristically reverse graded (McPhie *et al*, 1993). Debris flows are poorly sorted sediment and water slurries in which the slurry has sufficient strength to support large clasts during transport (Leeder, 1982; McPhie *et al*, 1993). Considered as a single unit, this bed coarsens upwards suggesting a grain flow, however the absence of smaller calcite clasts within the lower part of the unit suggests that it was not a single depositional event. Deposition is therefore likely to have occurred in several stages and may have been by debris flows or debris flows and grain flows in combination.

2.4 Discussion

The stratigraphy of the Bulgobac Falls area is dominated by mass flow sandstones of volcanic origin. The sandstone units contain abundant angular to sub-angular feldspar crystals and sub-rounded clasts of porphyritic andesites and basalts. With the exception of the lowest unit in the stratigraphy, there is an overall trend towards increasing quartz content within the sandstones upwards through the sequence. Where present, quartz crystals may be angular to sub-rounded and are often embayed supporting a volcanic origin. The angularity of the clasts suggests a proximal source.

A combination of mass flow processes is indicated. The calcareous volcaniclastic sandstone may have been deposited by debris flows and possibly grain flows, while the other sandstone and mudstone beds show clear evidence of deposition by turbidity currents. This suggests the sequence was deposited in a submarine environment below storm wave base. The depth for storm wave base in modern environments is highly variable, ranging from 10 to 200m (Reading, 1986 in White, 1996). There is an absence of sedimentary structures within the sequence, beyond the graded bedding and parallel laminations. Within the Bouma sequence (Fig 2.6a) it is possible to have wavy and ripple cross laminated sands. Although it is common for one or more stages of sequence to be absent from turbidites, it would be expected that they may be found on occasion. Such deposits are also usually syn-eruptive, as they are the result of slumping in unconsolidated deposits caused by earthquakes, explosive eruptions or sub-aerial flows generated by

similar events which transgress the shoreline (McPhie *et al*, 1993).

The presence of fossiliferous clasts within the calcareous volcaniclastic sandstone, suggests the source of the clasts was a shallow, near-shore environment during a hiatus in volcanic activity (Jago, 1972). The sandstone bed was probably in an environment close to the source environment, as the clast size does not suggest extensive transport

Chapter 3: Structural Geology

3.1 Introduction

The Bulgobac Falls area as mapped for this thesis is not structurally complex. This chapter documents the structural features of the area based on field measurement of bedding, cleavage and bedding-cleavage intersection lineation orientation. Particular attention was focused on evidence for a model developed by Kirsner (1992) which placed a significant NW-SE trending fault through the field area. Placement of this fault was based on an along strike change in magnetic character in the region (Fig 3.1).

3.2 Bedding and Cleavage

Beds within the area have a northeasterly strike and a westerly dip averaging 60° (Fig. 3.2a and 3.3). Two cleavages are evident, both closely spaced and smooth, one striking to the northeast and dipping steeply to the west and while the other has a shallower more northerly dip and strikes WNW. Both cleavages are weakly developed, appearing only occasionally in the finer grained sandstones and mudstones and not at all in the coarser grained units. The WNW striking cleavage was only found in near the axial plane of WNW trending parasitic folds. Figure 3.2b suggests the northeasterly striking cleavage to be the earlier cleavage as it has been folded by a deformation producing northwesterly trending folds.

3.3 Folding

The only folds found in the Bulgobac Falls area were small-scale parasitic folds in mudstone beds. These folds were observed to be NNE or WNW trending and shallowly plunging, approximately 30° and 40° respectively. These agreed with the cleavage/bedding intersection lineations, one with an average plunge of 30° towards 013 (S_0^S_2) and the other with an average plunge of 38° towards 285 (S_0 ^S_4) (Fig. 3.2c). All observed folds were gentle to open and upright to steeply inclined.

A synform to the west of the field area is indicated by the earlier cleavage dipping

more steeply than the bedding (McClay, 1987). The volcaniclastic mass flow units fine in a westerly direction, indicating younging, and confirming that the field area is on the eastern arm of a syncline (Fig.3.3). The stereonet of the poles to bedding (Fig. 3.2a) shows this syncline to be gently plunging to the NNE.

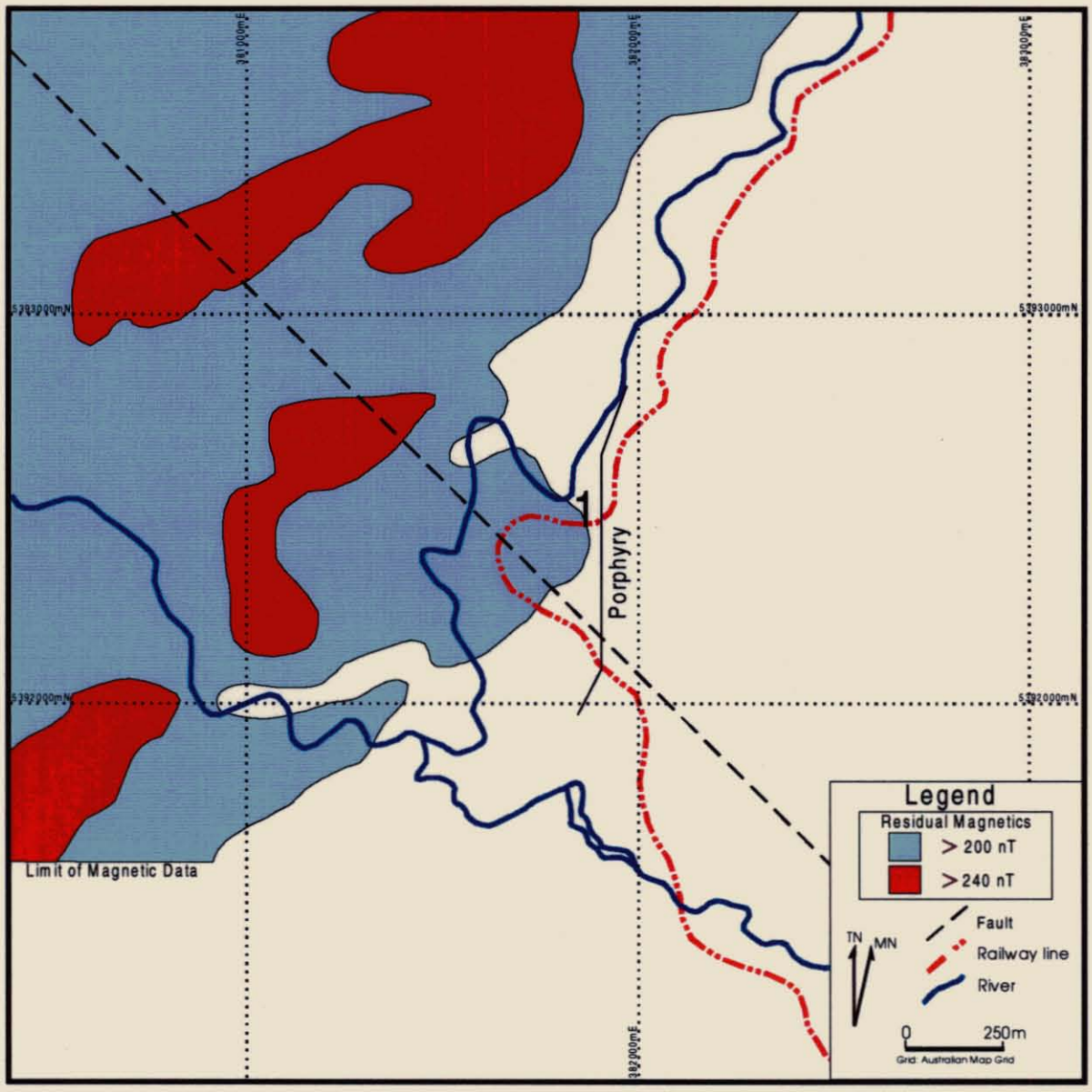

Figure 3.1: Outline of residual magnetic data for the Bulgobac Falls area, showing fault inferred from the magnetics (derived from Kirsner, 1992).

5 cm

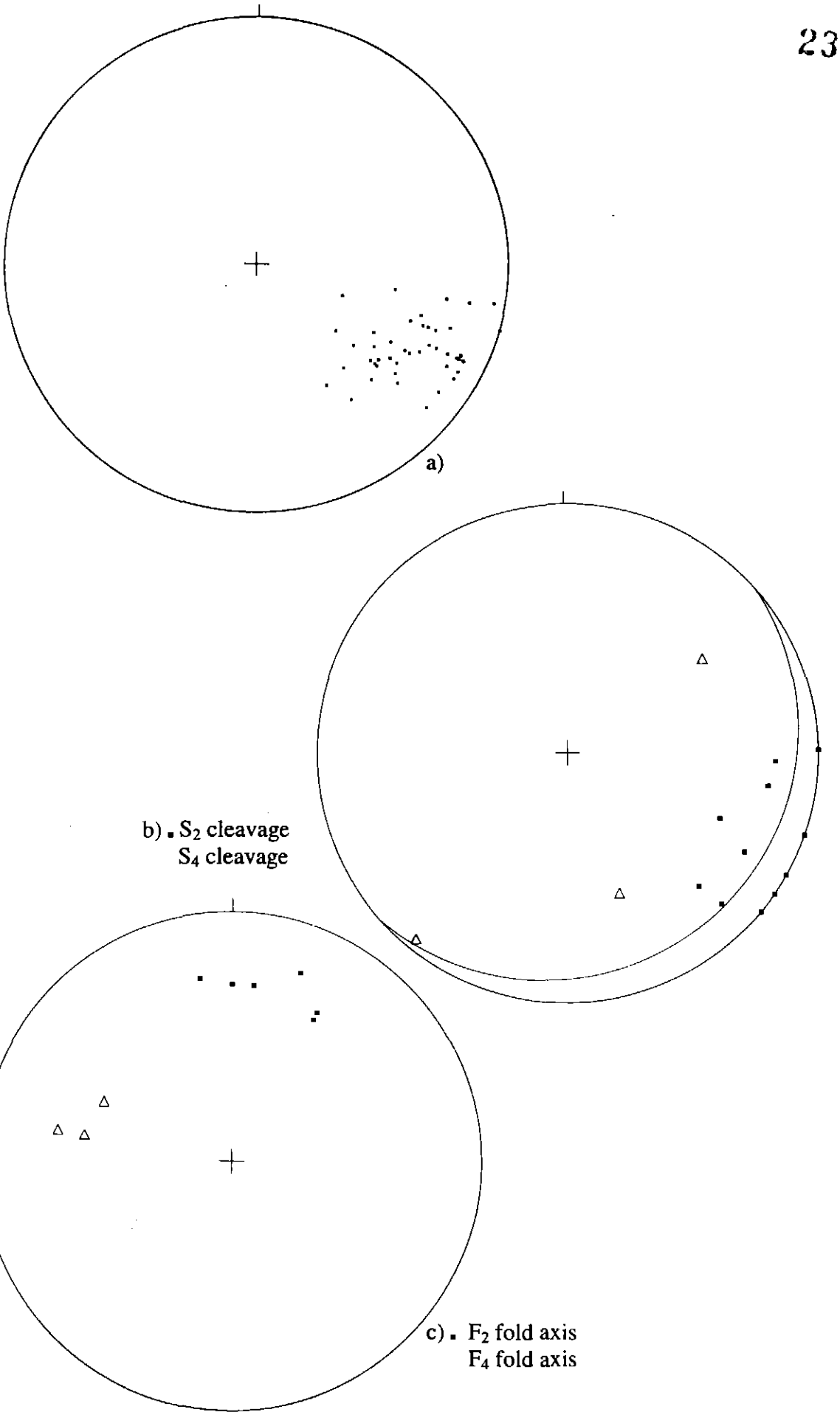

Figure 3.2: Stereonets of: a) poles to bedding b) poles to cleavage c) fold axis

3.4 Conclusion

Structural development in the Bulgobac Falls area is limited to two phases of deformation, producing gentle to open, upright to steeply inclined folds and associated axial planar cleavages. The folds are seen as parasitic folds in mudstones and an inferred regional syncline.

These folds are consistent with the structural sequence formed by deformation during the Devonian as described by Seymour (1980) and reviewed by Seymour and Calver (1995). Four deformation events are thought to have affected this region during that period (Table 3.1). The NNE trending folds are consistent with D_2 deformation caused by predominantly east-west convergence between uplifted Precambrian rocks of the Rocky Cape Block and the Tyennan Block (Fig. 3.4). Later compression from the northeast resulted in the Tyennan Block yielding to form the Cradle Mountain Block and the Prince of Wales Range Block (Williams *et al*, 1989). The resultant north-south trending folds of D_3 are not seen in this area, however the WNW trending folds are consistent with D_4 deformation.

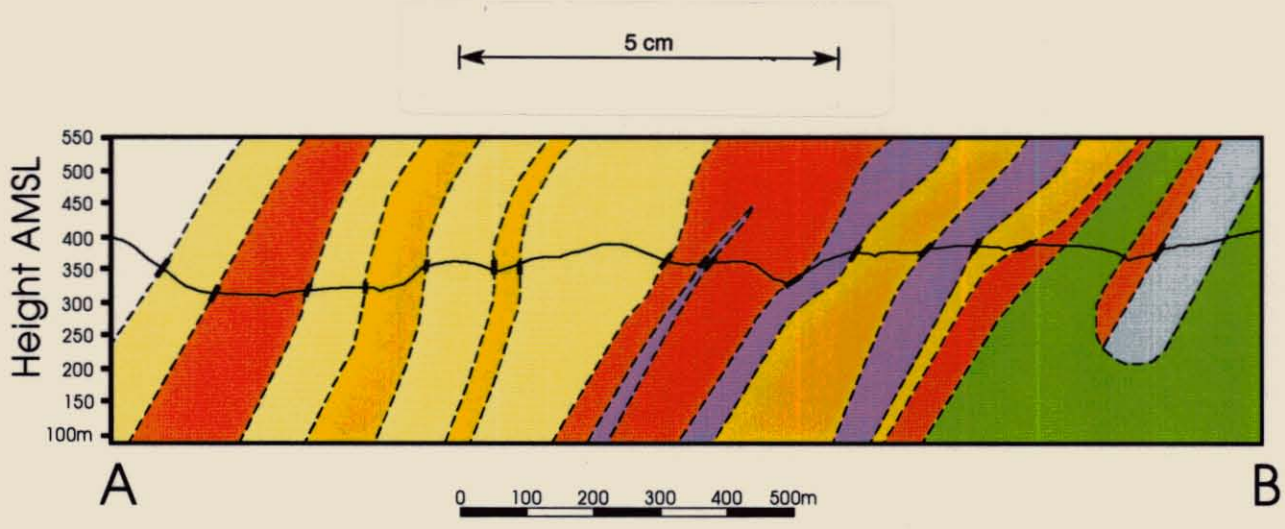

Figure 3.3: Cross section of the Bulgobac Falls area. Section line is shown on main map. Lithologies are as indicated by colours on main map.

No significant faults were observed within the Bulgobac Falls area. In particular, no evidence was found to support the model proposed by Kirsner (1992). This model suggested that the fault cut across strike through the Que River and the Emu Bay Railway. Outcrop was excellent in these areas, particularly along the rail line, and no evidence for displacement within these units or a change of lithology that might be attributed to a fault

was found. The reduction in magnetic signature at point 1 (Fig 3.1) can be accounted for by the cutting of the bedding by an intrusive porphyry. Reasons for the abrupt along strike drop in total magnetic intensity in units west of this will be discussed in chapter 5.

Phase	Trend	Style
D_4	NW-SE	Open to tight generally inclined folds with associated axial planar cleavage
D_3	N-S	Open to tight upright folds with associated axial planar cleavage
D_2	NE-SW	Open to tight upright to inclined folds with associated axial planar cleavage
D_1	E-W	Open upright folds with no cleavage development

Table 3.1: Devonian Structural Sequence (based on Seymour and Calver, 1995).

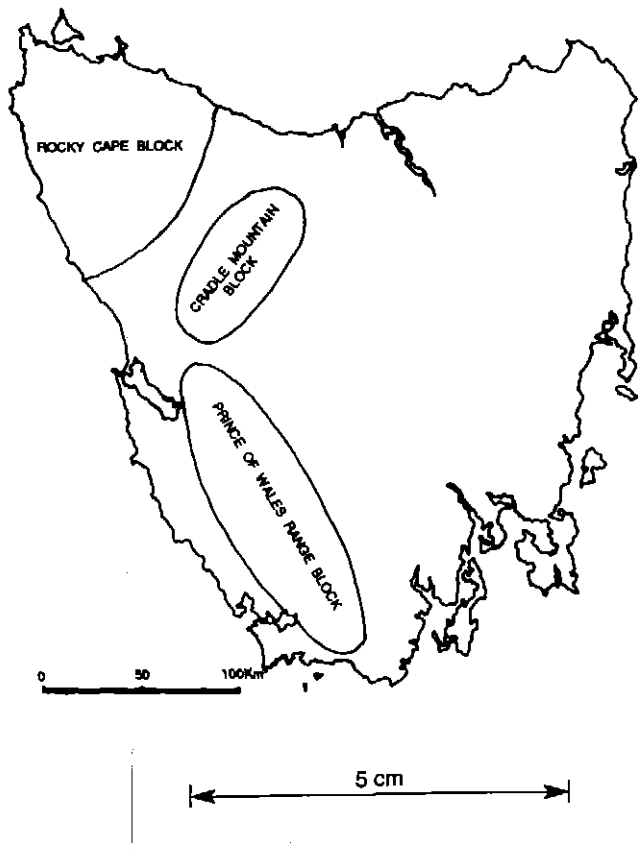

Figure 3.4: **Major** blocks associated with Devonian deformation in western Tasmania. Note that Cradle Mountain and Prince of Wales Range Blocks constituted the Tyennan Block during earlier Devonian deformation (Williams *et al*, 1989).

Chapter 4: Regional Correlations

4.1 Introduction

Stratigraphy is crucial in establishing a correlation between rock types in different areas. For rock units to be considered the same, or as correlates, they must be deposited at about the same time and have similar depositional environments and sedimentary sources. This will result in the development of similarities in the stratigraphy of both units. It will also lead to similarities in the geochemical composition of the rocks and their geophysical characteristics. To establish a correlation between the Tyndall Group, and therefore the Mount Cripps Subgroup, and the sequence at Bulgobac Falls, it is vital to show strong similarities in stratigraphy. Stratigraphic correlation will be the primary focus for this chapter, with supporting evidence from geophysics, whole rock geochemical analysis and carbon-oxygen isotope analysis of carbonate samples.

This work will also be used to define the stratigraphy, by establishing the subdivisions within it as clearly as possible. A correlation will also be made with local stratigraphic sequences to show that the sequence described fits within the local context and to enhance the understanding of the local geology.

4.2 Geophysical Correlation

The Lynchford Member can be distinguished from surrounding rocks by a characteristic high magnetic susceptibility due to its high titanomagnetite content (McKibben, 1993; White and McPhie, 1996). Magnetic susceptibility readings were taken on all coarser grained units in the field to aid in identification of the Lynchford Member correlate in the area and to compare these results with existing aeromagnetic data. A unit was considered to be highly magnetic if a reading in excess of 200×10^{-5}nT was obtained. These results showed highly magnetic units exist in the south of the area particularly, while the magnetic signature drops significantly to the north (Fig. 4.1). From the high magnetic signature of the rocks a correlation to the Lynchford Member can be made.

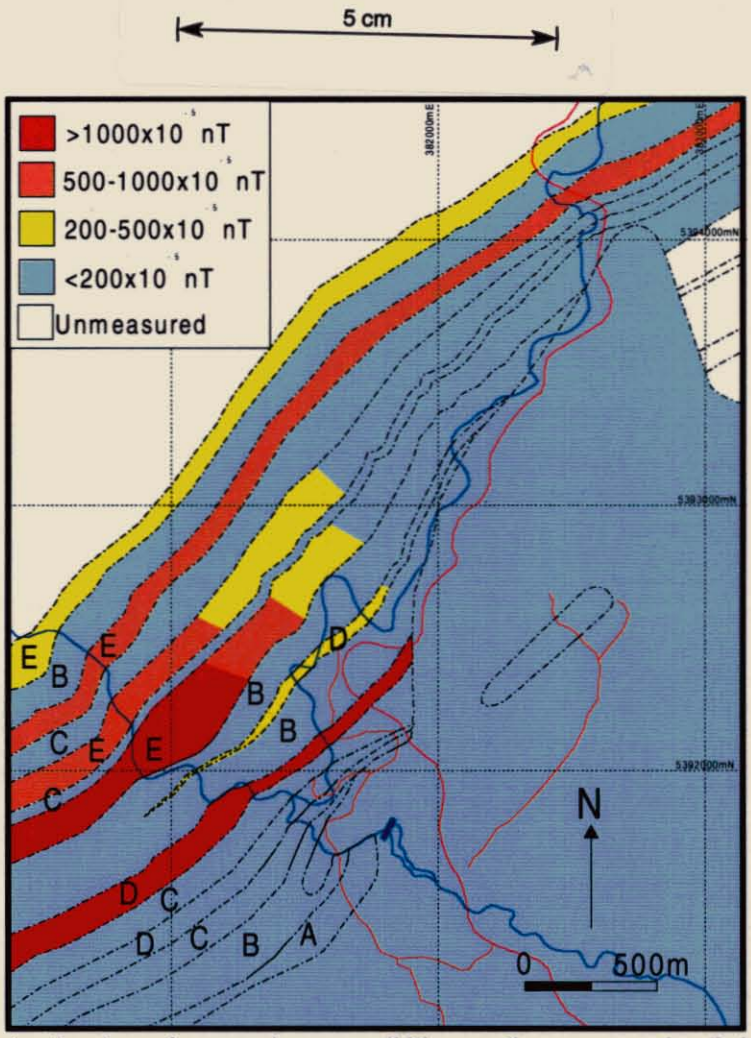

Figure 4.1: Schematic drawing of magnetic susceptibility readings across the Bulgobac Falls area. Lithological units are as indicated on main map. Along strike magnetic changes are based on isolated outcrop readings and variations are not necessarily sharp, nor are boundaries accurately indicated. Lithofacies: A – Calcareous volcaniclastic sandstone; B: - Laminated mudstone with fine sandstone; C – Interbedded mudstone and medium to coarse sandstone; D – Qtz-poor, crystal-rich volcaniclastic sandstone; E – Qtz-rich, crystal-rich volcaniclastic sandstone.

4.3 Stratigraphic Correlations

To avoid repetition, the quartz-poor crystal rich volcaniclastic sandstone facies and the quartz-rich crystal-rich volcaniclastic sandstone facies have been grouped where possible in this section, and are collectively referred to as the crystal-rich volcaniclastic sandstone.

4.3.1 Stratigraphy of the Tyndall group

The stratigraphic nomenclature of the Tyndall Group has been outlined in chapter 1. Poltock (1993) correlated the Bulgobac Falls stratigraphy to the lower Tyndall Group, based, in part, on lithological similarities and on the aeromagnetic data (Kirsner, 1992). It is this portion of the Tyndall Group stratigraphy, the Comstock Formation, that is the focus here.

White (1996) and White and McPhie (1996) have provided the most complete definitions of Tyndall Group stratigraphy thus far. They have defined the principle lithofacies of the Lynchford Member and the Mt Julia Member, as outlined in Table 4.1. Seven locations are used to describe Tyndall Group and the stratigraphy of its correlates (Fig. 4.2, locations 1-6 and 8).

	Principle Lithologies	Major Composition	Minor Composition	Matrix	Bed Description
Mt. Julia Member	Quartz-rich, crystal-rich volcaniclastic sandstone	quartz and plagioclase crystals	lithic clasts – mostly felsic volcanic titanomagnetite clinopyroxene	albite, chlorite and quartz-rich	massive, non-graded and normally graded
	Volcaniclastic lithic breccia/ sandstone	quartz and plagioclase crystals, breccia base: lithic clasts felsic +/- quartz volcanics	not described	not described	massive normally graded, breccia at base, grading to crystal sandstone
	Laminated mudstone and sandstone	not described	not described	quartz-feldspar altered in places	tabular, laminated, sandstones normally graded, fossiliferous in places
Lynchford Member	Quartz-poor crystal-rich volcaniclastic sandstone	crystals of plagioclase, clinopyroxene titanomagnetite +/- ilmenite	quartz, felsic to mafic volcanic lithic clasts	chlorite, albite and quartz rich	massive graded from pebbly sandstone to mudstone
	Laminated mudstone and sandstone	not described	not described	not described	parallel, laminated and graded, and massive black mudstone
	Volcaniclastic lithic breccia	lithic clasts angular, pebble to cobble sized	quartz	crystal and/or mud-rich	graded
	Carbonate	recrystallised calcite +/- hematite	chlorite sericite	not described	massive, fossiliferous (mid-late Cambrian)

Table 4.1: Principle lithofacies of Comstock Formation, more common facies occur higher in the table. Major composition is defined as 15% or more of total composition Note: the Mt Julia Member includes welded ignimbrites and coherent rhyolite/rhyolite breccia not included here as they do not aid in correlation (derived from White, 1996).

The most common facies within both members is the crystal-rich volcaniclastic sandstone. The Mount Julia Member has higher quartz content than the Lynchford Member and the crystal-rich volcaniclastic sandstone is even more dominant over the laminated mudstone and sandstone facies. Within the Lynchford Member, a subordinate quartz-rich crystal-

rich volcaniclastic sandstone is found at Lynchford and in the Anthony Road area. The Lynchford Member correlate from the Mount Cripps Subgroup at Cradle Mountain Link Road does not contain a crystal-rich volcaniclastic sandstone, and is instead dominated by laminated mudstones, with minor siliciclastic sandstone to conglomerate beds (Fig 4.1) (White, 1996).

White (1996) considers the crystal-rich volcaniclastic sandstones to have been deposited by high-density turbidity currents or debris flows. The laminated mudstone and sandstone facies was the result of low- to high-density turbidity flows and hemi-pelagic sedimentation.

The base of the Tyndall Group is not readily defined as the lithofacies do not have a consistent stratigraphic order. Where the quartz-poor crystal-rich volcaniclastic sandstone occurs, the base can be defined by its first occurrence. If the carbonate facies is present, it occurs at the base of the Lynchford Member and is overlain by the other facies (White, 1996).

4.3.2 Correlation of the Bulgobac Falls Sequence with the Tyndall Group

The sedimentary sequence in the Bulgobac Falls area has been divided here into five lithofacies, detailed in chapter 2 and summarised in Figure 4.2 and Table 4.2. It can be seen that three of these facies correlate well with the Comstock Formation as described by White (1996) and White and McPhie (1996).

Both the crystal-rich volcaniclastic sandstone facies in the Bulgobac Falls sequence have similar compositions and bed forms to the crystal-rich volcaniclastic facies within the Comstock Formation. The trend for increasing quartz content upwards through the stratigraphy observed in the Comstock Formation is also seen in the Bulgobac Falls sequence with the quartz-rich sandstone occurring higher in the stratigraphy than the quartz-poor sandstone (Fig. 4.2 and Map). The Bulgobac Falls sequence crystal-rich volcaniclastic sandstones are interpreted as having been deposited by high-density turbidity currents. A similar interpretation has been applied by White (1996) although he included debris flows as an alternative option.

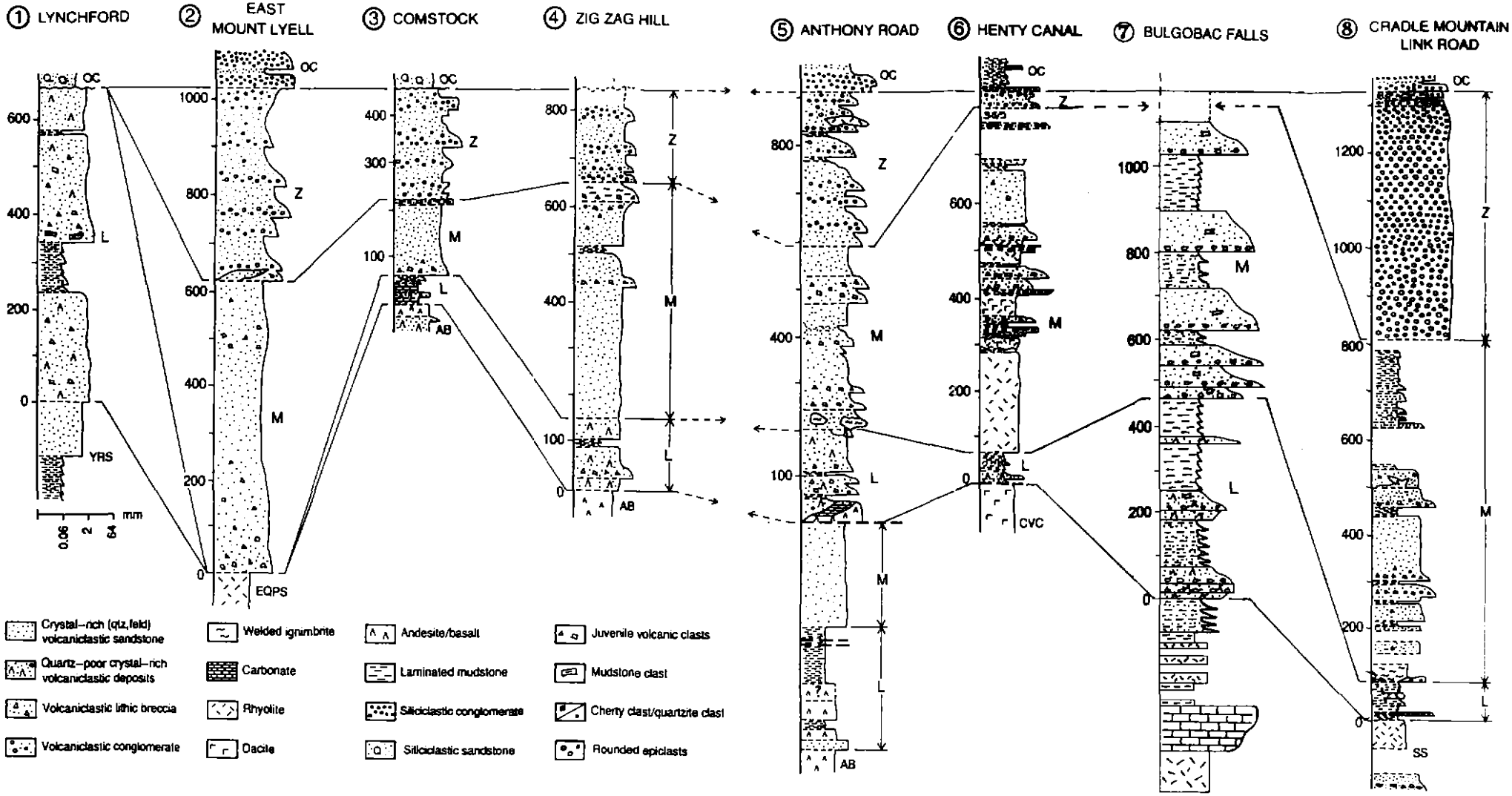

Figure 4.2: Correlation of the Bulgobac Falls sequence to seven key stratigraphic sections of the Tyndall Group. Subdivisions: L = Lynchford Member; M = Mt Julia Member; Z = Zig Zag Hill Formation. Underlying units include Yolande River Sequence (YRS), Eastern quartz-phyric sequence (EQPS), andesite and basalt units (AB), Central Volcanic Complex (CVC) and Southwell Subgroup (SS). Owen Conglomerate (OC) overlies the Tyndall Group. Approximate grid references (AMG) for the sections are as follows: Lynchford; 5337500N – 379520E (base) to 5337800N – 378960E (top): East Mt Lyell; 5342530N – 387400E (base) to 5343210N – 386270E (top): Comstock,; derived from drill holes Co72 and C59, collared around 534560N – 383130E: Zig Zag Hill; 5345910N – 381650E (base) to 5346500N – 382500E (top): Anthony Road; 5355900 – 380620E (base) to 5359200N – 381300E (top): Henty Canal; 5360700N – 379750E (base) to 5359750N – 380900E (top): Bulgobac Falls; 5391750N – 381750E (base) to 5392600N – 380550E (top): Cradle Mountain Link Road; 5398680N – 395260E (base) to 5399100N – 397480E (top)(modified from White, 1996).

Following White (1996) the Bulgobac Falls sequence is divided into a Lynchford Member correlate and a Mount Julia Member correlate based on the first occurrence of the quartz-rich, crystal-rich volcaniclastic sandstone facies (Fig. 4.2). This marks the lowest point in the stratigraphy that can clearly be considered to be part of the Mount Julia Member. The absence of further beds of the quartz-poor, crystal-rich volcaniclastic sandstone above this point supports this conclusion, as does the laminated mudstone bearing facies becoming less prevalent.

The Bulgobac Falls sequence crystal-rich volcaniclastics also include clasts of metamorphic rocks, particularly quartz-rich mica-schists and quartzites, that are not seen in other Tyndall Group crystal-rich volcaniclastic sandstones.

Principle Lithologies	Major Composition	Minor Composition	Matrix	Bed Description
Quartz-rich crystal-rich volcaniclastic sandstone	feldspar and quartz crystals	lithic clasts; felsic-mafic volcanics, metamorphics	chlorite-rich	normally graded from pebbly base
Quartz-poor crystal-rich volcaniclastic sandstone	feldspar clinopyroxene and magnetite crystals	quartz, lithic clasts felsic –mafic volcanics, metamorphics	chlorite-rich	normally graded from pebbly base and reverse graded
Interbedded mudstone and medium-coarse sandstone	not described	not described	not described	sandstones normally graded to mudstone
Laminated mudstone with fine sandstone layers	not described	quartz within sandy layers	sericite and chlorite rich	thinly bedded, sandstones normally graded
Calcareous volcaniclastic sandstone	micritic and sparry calcite clasts, calcite, feldspar and quartz crystals	lithic clasts; rhyolitic volcanics	sericite, chlorite and carbonate rich	massive, poorly sorted possibly reverse graded, fossiliferous clasts

Table 4.2: Principle lithofacies of the Bulgobac Falls sequence. More common facies occur higher in the table and major composition is defined as 15% or more of total rock composition

A comparison of laminated mudstone and sandstone facies in Tables 4.1 and 4.2 shows there is a strong correlation between the Bulgobac Falls sequence and the Tyndall Group. In the Tyndall Group, this facies includes fine sandstone beds up to "tens of centimetres" thick and medium to coarse sandstone beds which are up to 3 metres thick (White, 1996). This suggests that the interbedded medium to coarse sandstone and mudstone facies described within the Bulgobac Falls area can be correlated with the Tyndall Group

laminated mudstone and sandstone facies as well. The interbedded medium to coarse sandstone facies within the Bulgobac Falls sequence contains beds up to 1.5 metres thick, while the laminated mudstone facies includes sandstone beds that are up to 45 cm. thick. There are no massive black mudstone beds found in the Bulgobac Falls area.

The laminated mudstone facies of the Bulgobac Falls sequence is interpreted as having been deposited by low-density turbidity currents, while the interbedded mudstone and medium to coarse sandstone facies is considered to have been deposited by higher intensity turbidity currents. Combining these two facies provides a good correlation with White's (1996) interpretation for a depositional environment for the laminated mudstone and sandstone facies of the Comstock Formation as discussed in 4.2.1. The hemi-pelagic sedimentation included in White's (1996) interpretation was related to the massive black mudstone deposits found in some sections of the Comstock Formation, but not seen in the Bulgobac Falls area.

It is not possible to correlate the carbonate facies of the Comstock Formation with the calcareous volcaniclastic sandstone of the Bulgobac Falls sequence as the carbonate facies is considered to be massive and *in situ* (Jago, 1972). The Bulgobac Falls sequence is clearly a calcareous sandstone with bouldery carbonate clasts, which are clearly sourced from another area. Jago and McNeill (1997) reported similar limestone clasts within a mass flow unit of the Southwell Subgroup in a drill hole approximately 20km northeast of the Bulgobac Falls area. These clasts also contain trilobite fossils of the genus *Amphoton* and are contained in a volcaniclastic cobble conglomerate. Current drilling by Aberfoyle Resources Ltd. around that area has also found two horizons within the Southwell Subgroup that contain non-fossiliferous carbonate clasts (A. McNeill, pers. comm.,1997)

The Bulgobac Falls sequence can be seen to correlate well with Tyndall Group stratigraphy when comparing the facies found in the area with Tyndall Group facies, depositional styles and with the overall stratigraphic trend through the Comstock Formation. There are however differences seen in the Bulgobac Falls sequence which do not detract from correlation with the Tyndall Group, but are worthy of note.

Analysis of Figure 4.2 shows that the Bulgobac Falls sequence is considerably thicker than Tyndall Group sequences seen elsewhere. Within the described stratigraphies, the Tyndall

Group and its correlates vary from under 500m thick at Comstock to over 1300m thick at Cradle Mountain Link Road. The mapped portion of the stratigraphy within the Bulgobac Falls area is 1100m thick and does not represent the complete sequence within the area. The upper boundary of the Mount Julia Member has not been determined, nor has the existence or, if present, the thickness of the Zig Zag Hill Formation.

A second significant difference within the Bulgobac Falls sequence is the greater significance of the mudstone facies. The laminated mudstone facies dominates the Lynchford Member only in regions where the Lynchford Member is less than 100m thick and is a minor facies within the Mount Julia Member. Within the Bulgobac Falls sequence mudstone containing facies dominate the Lynchford Member correlate and form a significant proportion of the Mount Julia Member correlate (Fig. 4.2). The only other sequence in which the mudstone facies forms a significant portion of the Mount Julia Member is within the Mount Cripps Subgroup at the Cradle Mountain Link Road (Fig 4.1). This may suggest a greater proportion of mudstone within the Mount Julia Member correlate is a feature of the Mount Cripps Subgroup, however the link is tenuous at this stage with only two stratigraphic columns used for comparison.

In further attempting to correlate the Bulgobac Falls sequence to the Mount Cripps Subgroup, it is necessary to compare the Lynchford Member correlate at the Cradle Mountain Link Road with the lower stratigraphy in the Bulgobac Falls area. At least superficially from the stratigraphic columns (Fig 4.1) there does not appear to be much similarity. On the Cradle Mountain Link Road, The Lynchford Member correlate is thin, predominantly laminated mudstone facies and includes a siliciclastic conglomerate not seen in the Bulgobac Falls sequence. The siliciclastic conglomerate includes abundant Precambrian derived quartzite and muscovite schist and minor felsic volcanics (Pemberton *et al*, 1991). This is a clast type not reported to have been seen within the Lynchford Member (White, 1996). However it does occur as a minor component within the Bulgobac Falls sequence and suggests a common Precambrian basement source for the Lynchford Member correlates within the Mount Cripps Subgroup. The variation between the Cradle Mountain Link Road and the Bulgobac Falls area suggests the Bulgobac Falls sequence represents deposition in a transitional environment between a region with siliceous basement and felsic volcanics source rocks and regions with a higher proportion of intermediate to mafic source rocks.

4.4 Geochemical Correlations

4.4.1 Whole Rock Geochemical Analysis of the Mount Read Volcanics

Recent work by Berry *et al* (1997) has shown that Tyndall Group volcaniclastic rocks have a distinctive geochemical signature. They have used spider diagrams to compare the geochemical signature of different sandstones within the Mount Read Volcanics. normalised to Post Archaean Australian Shale (PAAS) of Taylor and McClennan (1985), rocks of tholeiitic origin have positive Ti, P and Nb anomalies due to the PAAS having a weak calc-alkaline signature. The PAAS represents an average granodioritic composition, and as such, rocks of mafic origin will have a positive slope towards the relatively enriched compatible element abundances on the right of the spider diagrams. Rocks of more felsic composition have a negative slope.

In analysing volcaniclastic sandstones from the Tyndall Group by this method, several characteristic features have been found. Samples analysed from the Lynchford Member (Fig. 4.3a) show a high Ti/Th ratio, have an overall mafic signature by virtue of a positive slope to the right and show very low Th values and high Sc values. There are also no negative Nb, P or Ti anomalies in contrast to most volcaniclastic rocks within the Mount Read Volcanics. Other Tyndall Group volcaniclastics (Fig 4.2b) do not show such distinctive characteristics, but do show the positive slope to the right and lack the negative Nb anomaly (Berry *et al*, 1997).

4.4.2 Whole Rock Geochemical Analysis of the Bulgobac Falls Sequence

To enable a correlation with other Tyndall Group whole rock geochemical signatures, samples of the crystal-rich volcaniclastic sandstones were analysed from across the stratigraphy. Samples were also taken along strike, to aid in correlating the relatively isolated outcrops throughout the area and further examine evidence for the fault postulated by Pasminco (Kirsner, 1992) and discussed in chapter 3.

The results were initially plotted on the premise that the Mount Cripps Subgroup begins at the units with the high magnetic signature. This plot showed that the rocks from this unit and above correlate well with Tyndall Group volcaniclastic sandstones (Fig. 4.4). Within

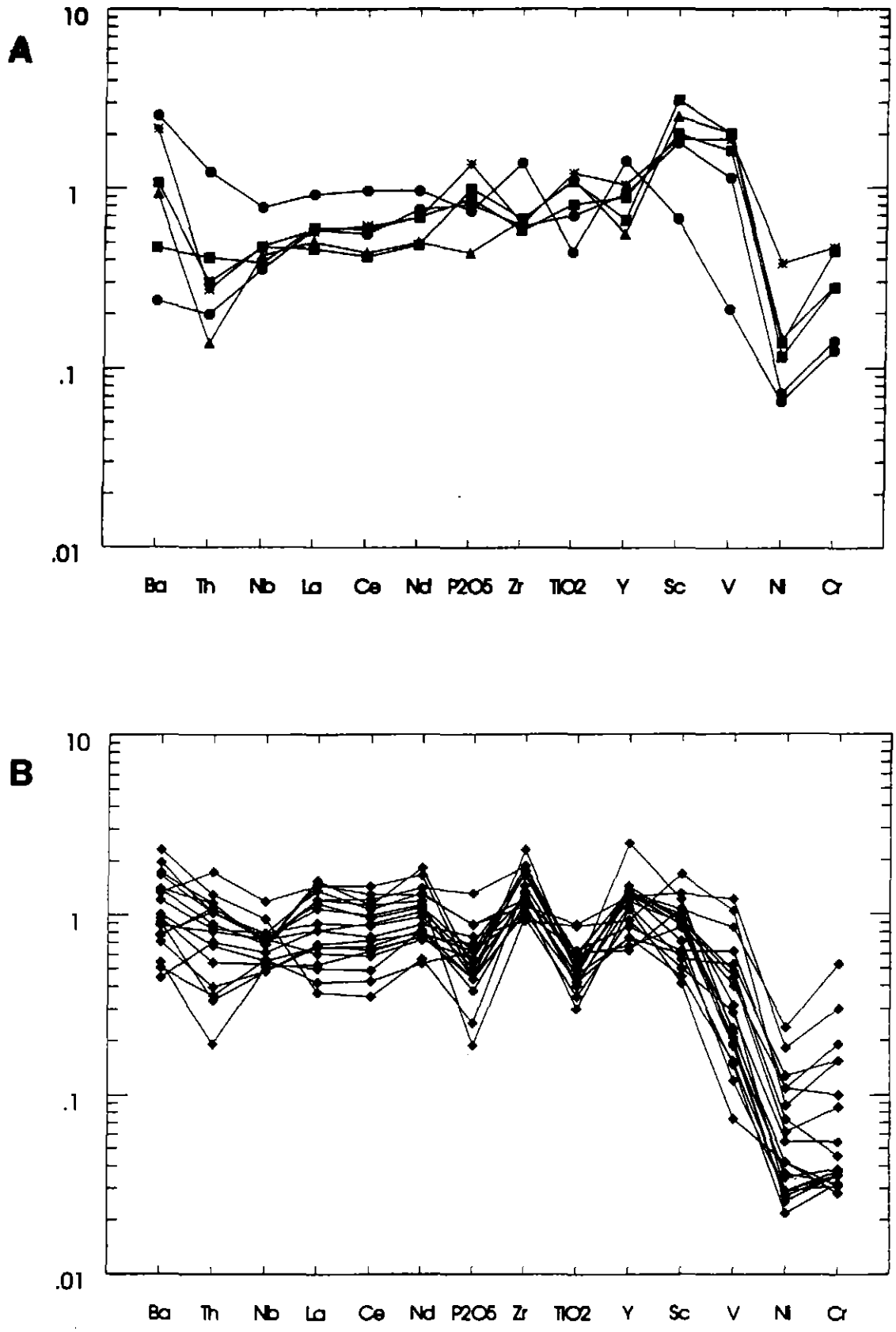

Figure 4.3: Spider diagrams normalised to PAAS (Taylor and McClennan, 1985) for Tyndall Group volcaniclastics. a) Lynchford Member b) Younger Tyndall Group (Berry *et al*, 1997)

this portion of the stratigraphy, there is no negative Nb, Ti or P anomaly, the Ti/Th ratio is high due to the low Th and the lack of depletion of Ti and there is an overall positive slope on the spider diagram. When the results of the analysis of the samples taken along strike in the north of the field area are added (Fig 4.5), it can be seen that these rocks match the Lynchford member pattern of the diagram well and confirm the field, hand specimen and thin section correlation of these rocks to the southern portion of the Bulgobac Falls sequence. This further supports the conclusion from chapter 3 that there is no evidence for a major northwest trending fault displacing the stratigraphy within the area.

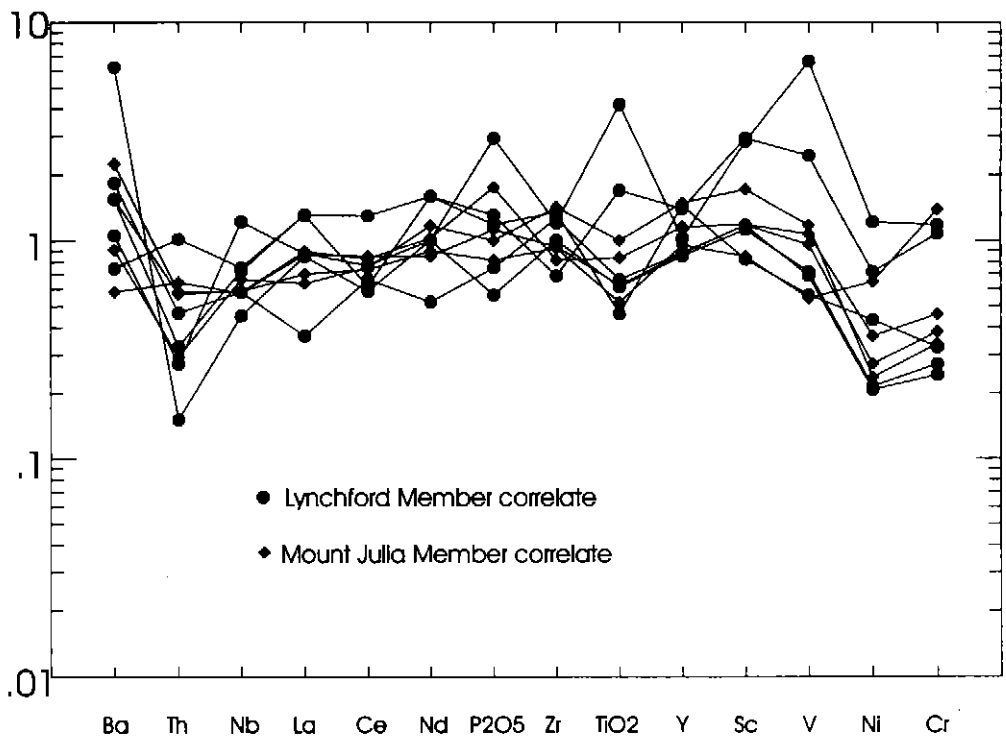

Figure 4.4: Spidergram normalised to Post Archaean Australia shales (PAAS, Taylor and McLennan, 1985) of highly magnetic crystal-rich volcaniclastic sandstones from the Bulgobac Falls sequence. The separation into Lynchford Member and Mount Julia Member is as suggested in Fig. 4.2.

As has been shown in Figure 4.1, the magnetic units start at the second unit of facies D. Two volcaniclastic sandstone units occur below the magnetic units. Stratigraphic analysis has already correlated the higher of these to facies D and hence to the Mount Cripps Subgroup, while the calcareous sandstone has been suggested to be part of the Southwell Subgroup (see map). When the results from these units are added to the spider diagram (Fig. 4.6), the upper unit is indistinguishable from the overall pattern of the more magnetic

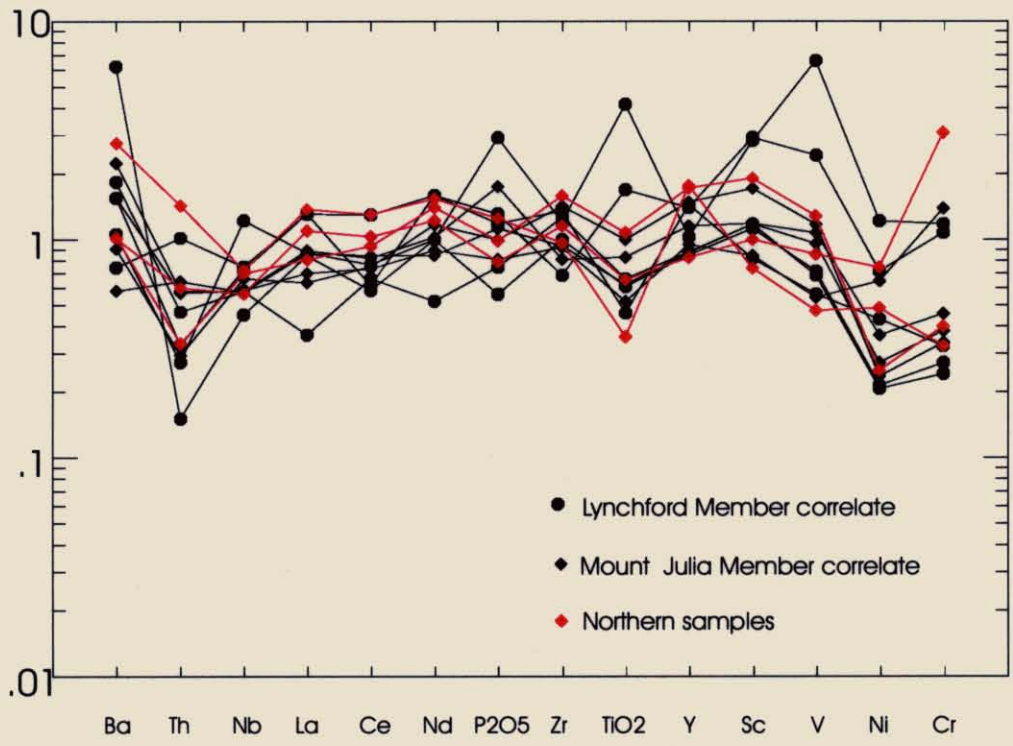

Figure4.5: Spidergram normalised to Post Archaean Australia shales (PAAS, Taylor and McLennan, 1985) of highly magnetic crystal-rich volcaniclastic sandstones with the less magnetic northern units from the Bulgobac Falls sequence.

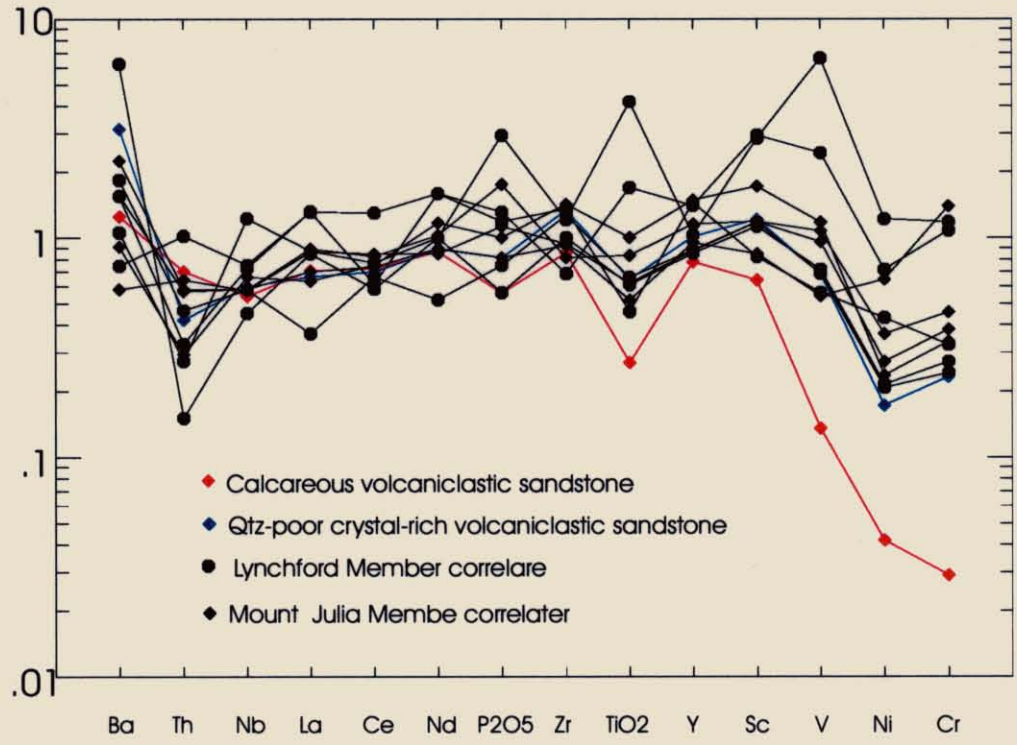

Figure 4.6: Spidergram normalised to Post Archaean Australia shales (PAAS, Taylor and McLennan, 1985) of highly magnetic crystal-rich volcaniclastic sandstones with the stratigraphically lower less magnetic units from the Bulgobac Falls sequence.

units, while the calcareous sandstone has a slight depletion in Nb and P, a low Ti value, a low Ti/Th ratio and a negative slope. Whilst the pattern is not particularly strong and it is difficult to base a clear conclusion on the results from a single unit for this type of analysis, it does strengthen the existing stratigraphic conclusion that this unit is part of the Southwell Subgroup. The first quartz-poor crystal-rich volcaniclastic sandstone unit clearly correlates with the overlying units and is therefore interpreted here as the base of the Mount Cripps Subgroup.

4.4.3 The Limestone Clasts

Samples were taken from the calcite clasts at the top of the calcareous volcaniclastic sandstone for carbon and oxygen isotope analysis. Both the micritic calcite and the sparry calcite layers were sampled (Table 4.3). Figure 4.7 shows that these samples plot within and close to the range of Tyndall Group carbonates found at Comstock, and close to and within the field of worldwide Cambrian sedimentary carbonates. A sedimentary origin is therefore likely for the calcite clasts found within the calcareous volcaniclastic sandstone although MacDonald (1991) considered it possible for the Comstock carbonate to have had hydrothermal origins.

Sample	d13C (wrt PDB)	d18O (wrt PDB)	d18O (wrt SMOW)
Micritic calcite (P19A)	1.042	-16.632	13.715
Sparry calcite (P19B)	0.83	-13.745	16.691

Table 4.3: Results of the carbon and oxygen isotope analysis

4.5 Local Correlations

4.5.1 Aeromagnetic Data

Regional aeromagnetic mapping (Kirsner, 1992) shows a 2.5 km wide magnetic high extending along strike to the southwest of the Bulgobac Falls area for 5 km. On the eastern side of this two ridges of high magnetics are seen, the most easterly of these dies out south of the Bulgobac Falls area. The second ridge continues into the area and clearly corresponds to the highly magnetic bed indicated in Figure 4.1. This ridge is abruptly truncated in the south of the area, corresponding to the point at which the intrusive porphyry cuts that unit.

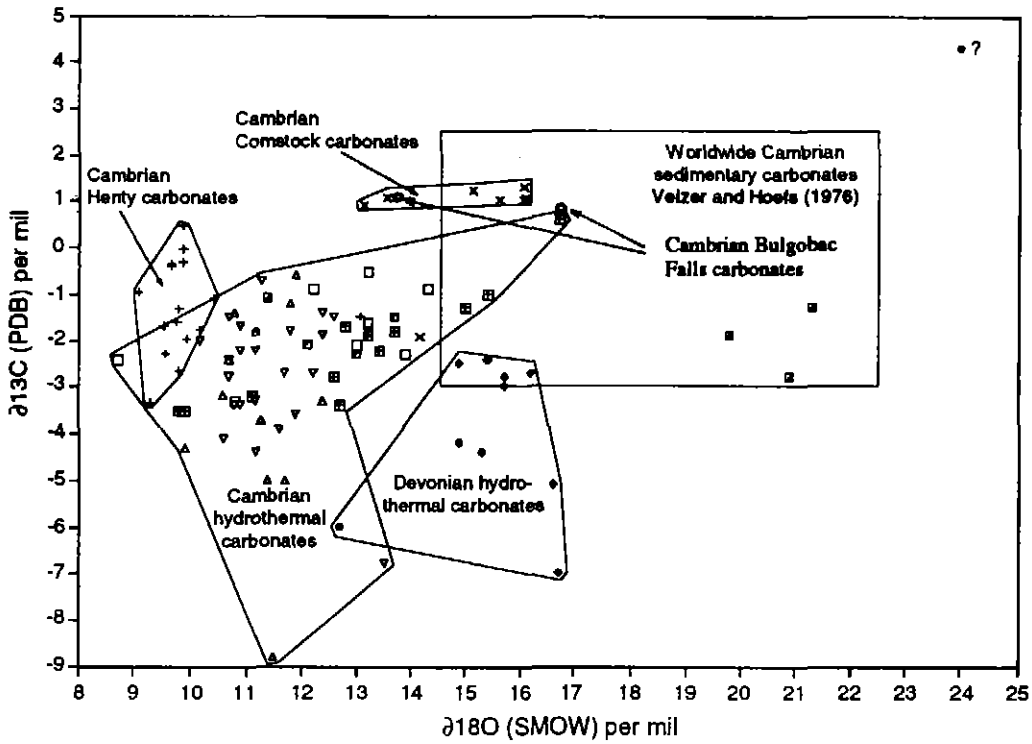

Cambrian Carbonates

- Comstock (data from MacDonald 1991)
- Henty (data from Yeats 1989)
- North Rosebery (data from Khin Zaw 1991, Dixon 1980)
- South Rosebery (data from Khin Zaw 1991, Dixon 1980)
- Hercules (data from Khin Zaw 1991)
- South Hercules (data from Khin Zaw 1991)
- Cleveland (data from Collins 1981)
- Renison dolomite (data from Patterson et al. 1981)

Devonian Carbonates

- Renison Devonian (data from Patterson et al. 1981)
- Cleveland Devonian (data from Collins 1981)

Figure 4.7: Bivariate diagram for d18O versus d13C showing fields for the Cambrian Henty and Comstock carbonates and the Bulgobac Falls carbonate clasts. Also shown is the field for worldwide Cambrian marine carbonates analysed by Veizer and Hoefs (1976), Cambrian hydrothermal carbonates of western Tasmania and Devonian hydrothermal carbonates of western Tasmania (adapted from White, 1996).

The southern end of the magnetically high region is in the Pinnacles area. At this point the ridges swing to the west, before dying out rapidly shortly after. This corresponds to the hinge of a syncline mapped in this region (Collins, 1980; Kirsner, 1992; McKibben, 1993). The remainder of the magnetically high area, is one of broad anomalies, and the along strike ridges of the eastern margin do not reappear to the west. This has been interpreted as being the result of truncation of the western side of the syncline by the Rosebery fault (Kirsner, 1992; Poltock, 1993).

Poltock (1993) has correlated the continuous magnetic high to a thin bed of mafic sandstone mapped by McKibben (1993) (Fig. 4.8). I have interpreted this bed to correspond to the eastern-most magnetic ridge based on a closer correlation between the position of the bed and the magnetic high in the Pinnacles area. This is supported by field descriptions discussed in the next section. The bed is continuous with the basal bed of the Mount Cripps Subgroup in the Bulgobac Falls area, however it loses its highly magnetic character between the two areas. The continuous magnetic ridge runs from the mafic sandstone at the core of the syncline (McKibben 1993) to the first highly magnetic bed in the Bulgobac Falls area (Fig. 4.8).

4.5.2 The Pinnacles

McKibben (1993) mapped the geology of the Pinnacles area approximately 5km southwest of the Bulgobac Falls area (Fig. 4.8). He describes the sedimentary sequence within this area as part of the Mt Charter Group, dominantly Southwell Subgroup. The hinge of the

syncline to the west of the Pinnacles area contains two beds of mafic sandstones. The map accompanying McKibben's (1993) thesis appears to show only one mafic bearing sandstone, however analysis of his text and data suggests the thin bed folded around the syncline and mapped as crystal + lithic +pumice rich mass flow was intended to be mapped as a mafic bearing sandstone.

The mafic bearing sandstone is described in hand specimen as green-grey, and in thin section as dominated by sericite-carbonate altered feldspar, pyroxene and felsic volcanic lithics, with minor quartz. This bed was correlated to the Tyndall Group and as such, described as the base of the Mount Cripps Subgroup (McKibben, 1993).

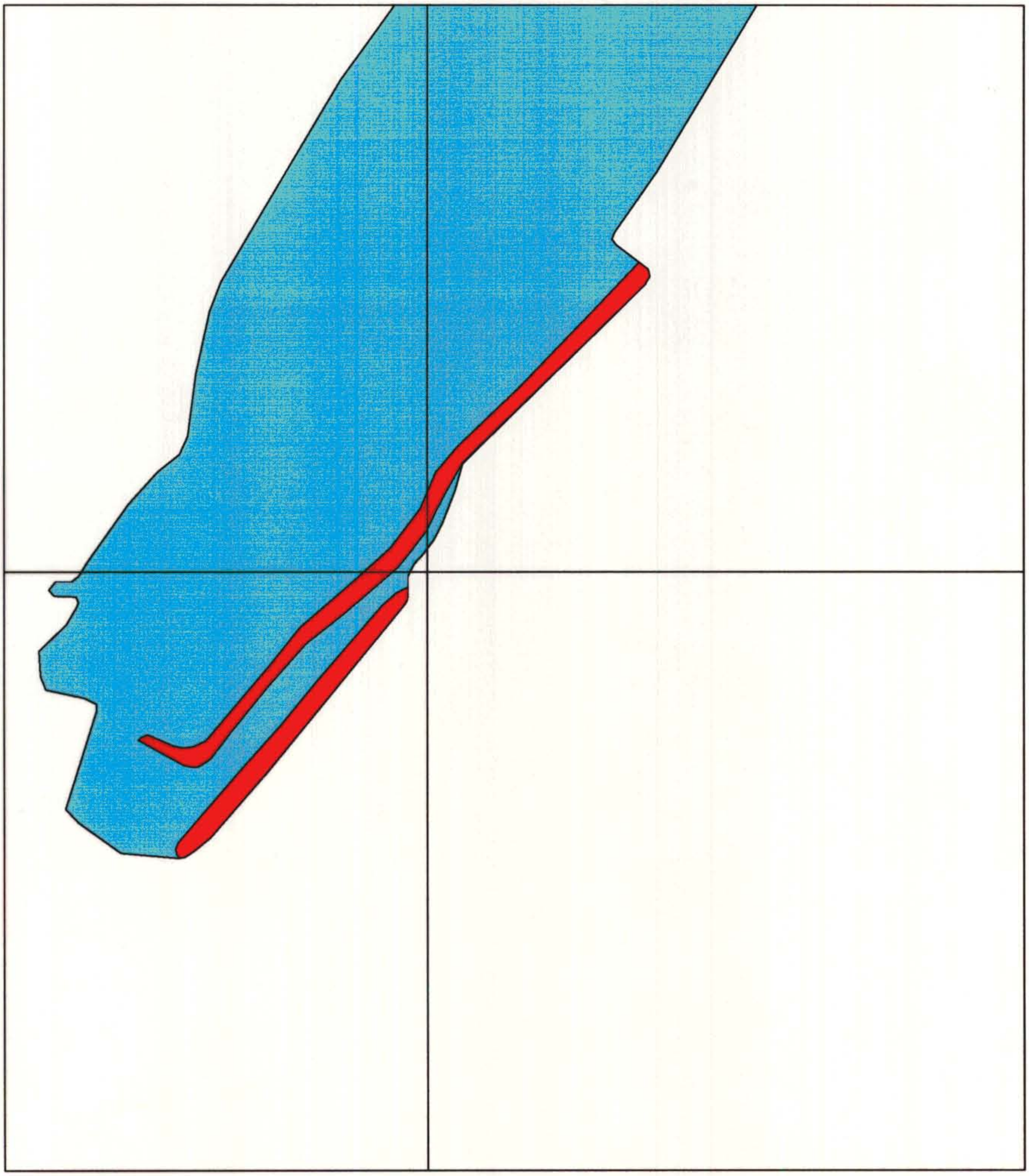

239055

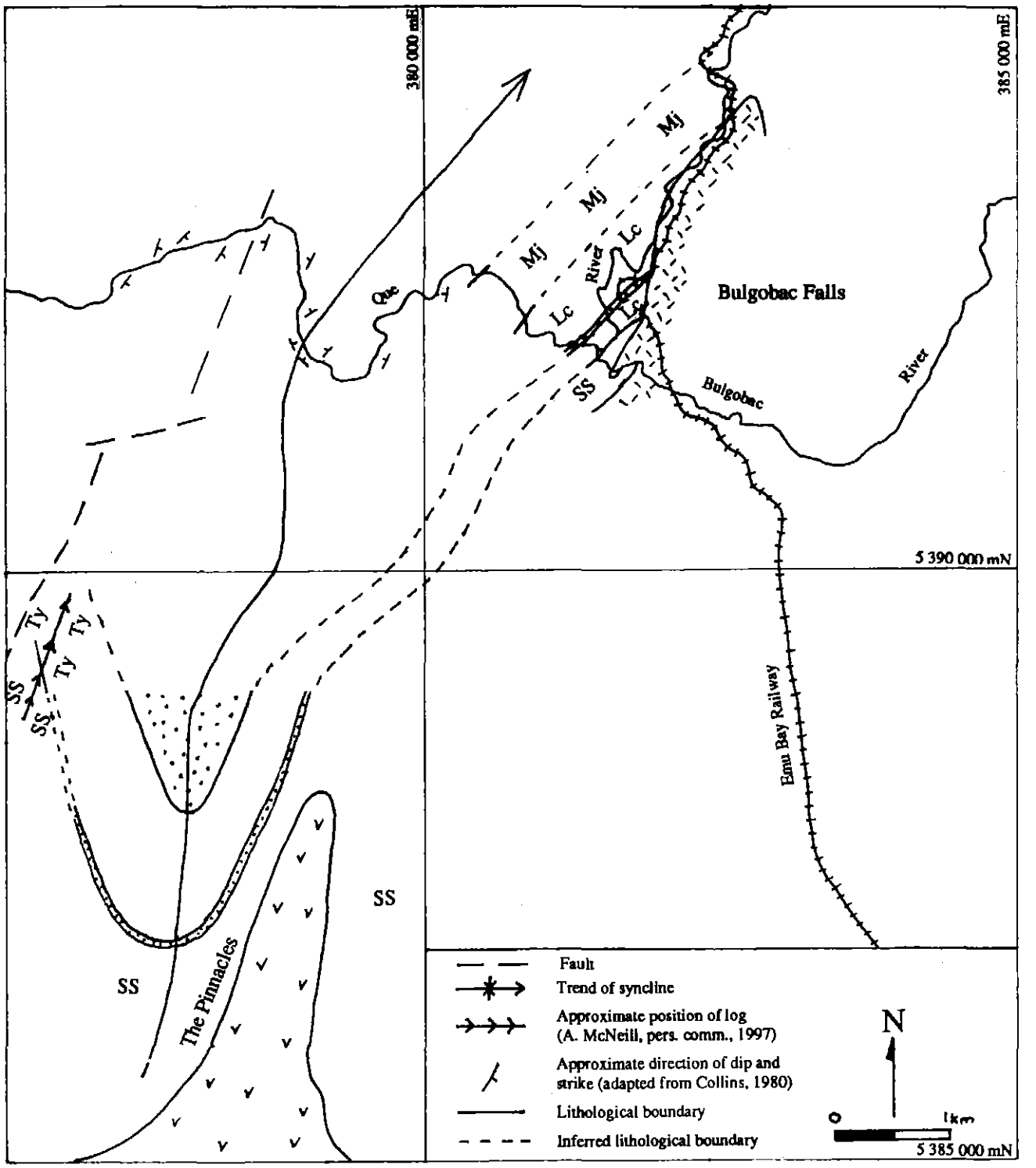

Quartz-feldspar porphyry

Pinnacles rhyolite (McKibben, 1993)

Mafic sandstone (inc. data from McKibben, 1993)

Lc Lynchford Member correlate

Mj Mt Julia Member correlate

Ty Tyndall Group correlate (A. McNeill, pers. comm., 1997)

SS Southwell Subgroup (inc. data from McKibben, 1993 and A. McNeill, pers. comm., 1997)

Figure 4.8: Map correlating the Bulgobac Falls stratigraphy with the Pinnacles stratigraphy, and showing the regional NNE trending syncline. The overlay is a schematic of the aeromagnetic data from Kirsner (1992) showing the linear magnetic highs (in red) on the eastern side of an area showing a moderated broad high (indicated in blue). No inference is intended as to actual magnetic values. Sources are indicated in legend.

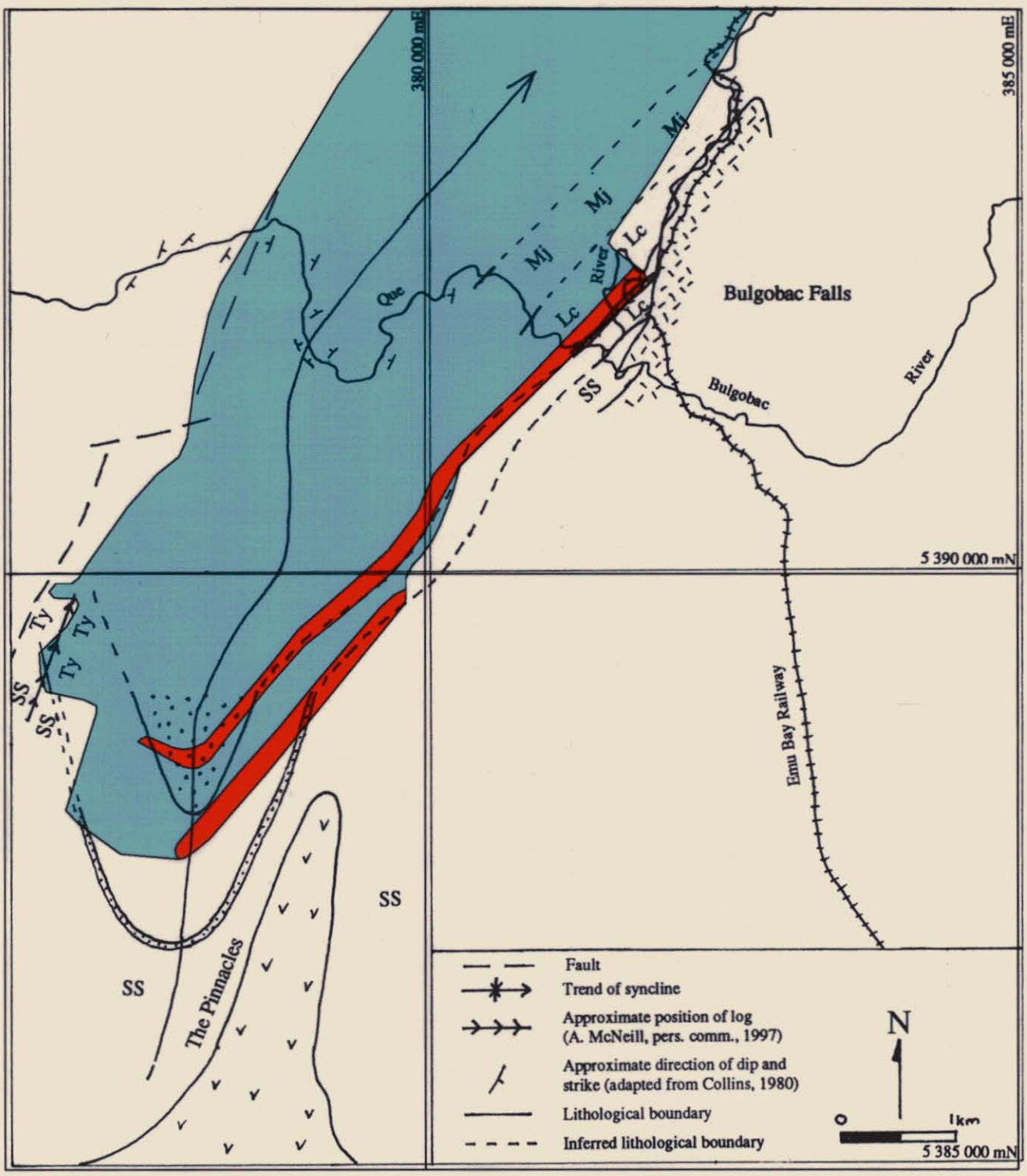

Quartz-feldspar porphyry

Pinnacles rhyolite (McKibben, 1993)

Mafic sandstone (inc. data from McKibben, 1993)

Lc Lynchford Member correlate

Mj Mt Julia Member correlate

Ty Tyndall Group correlate (A. McNeill, pers. comm., 1997)

SS Southwell Subgroup (inc. data from McKibben, 1993 and A. McNeill, pers. comm., 1997)

Figure 4.8: Map correlating the Bulgobac Falls stratigraphy with the Pinnacles stratigraphy, and showing the regional NNE trending syncline. The overlay is a schematic of the aeromagnetic data from Kirsner (1992) showing the linear magnetic highs (in red) on the eastern side of an area showing a moderated broad high (indicated in blue). No inference is intended as to actual magnetic values. Sources are indicated

Mapping by Aberfoyle Resources Ltd. approximately 2 km northwest of the Pinnacles area has shown the sequence within this area to include the base of the Mt Cripps Subgroup (Fig. 4.8; Appendix) (A. McNeill, Pers. Comm.). The contact described is along strike from the basal bed in the Pinnacles area and can be readily correlated to the western arm of the syncline described above. The aeromagnetic data shows a significant drop in magnetics along the line of this correlation however, before returning to a high level which correlates with the Aberfoyle mapping. This drop in magnetics may be due to faulting as was interpreted by Kirsner (1992) or it could be due to alteration of the rock composition. Faulting seems a more likely prospect however due to the proximity of the Rosebery fault and the abruptness of the change and rapid return to the regional magnetic trend.

4.5.3 The Silver Falls Syncline

The significant structure affecting the Mt. Cripps Subgroup in the local (as considered for this section) area is the north to northeast trending syncline, informally referred to as the Silver Falls Syncline (Poltock, 1993). The correlation of the Mt. Cripps Subgroup between the Pinnacles and the Bulgobac Falls area, shows that this structure is continuous between these areas on its eastern limb. The western limb appears truncated by the Rosebery fault shortly after folding around its axis in the Pinnacles area.

In attempting to trace the axial plane of the syncline, use was made of mapping data compiled by Collins (1980) along the Que River west of the field area, the aeromagnetic data (Kirsner, 1992) and tracing of the Rosebery fault by Poltock (1993). Two points along the Que River show changes of dip consistent with the axial plane of the syncline. At approximately 378500mE, the regional trend of bedding changes from westerly dipping to easterly dipping which could be indicative of the hinge of the syncline, however this also corresponds to a transition into a magnetically quiet zone. Were this to be the hinge of the syncline, it might be expected that the magnetic pattern to the east of this point would be repeated to the west. Poltock (1993) has mapped the Rosebery fault through this region and Owen Conglomerate correlates to the west of this. The change in dip could then be explained by the fault having brought an easterly dipping sequence into contact with the westerly dipping continuation of the Bulgobac Falls sequence.

Approximately 1 km southeast of this, is an area on the Que River where the dip changes temporarily to a shallow (20^0-25^0) NNE trend before rapidly returning to a steep westerly

dip. This would be consistent with the hinge of the fold which has been shown to have a NNE trending axial plane plunging at around 30^0. Dips to the west of the hinge would be expected to become easterly in this case. However if the fault is close to this region, the continuation of a westerly dip beyond the fold hinge could be a result of the close proximity of the fault.

4.5 Conclusions

A clear correlation has been established between the Bulgobac Falls sequence and the Comstock Formation, the lower formation of the Tyndall Group. The Bulgobac Falls sequence has similar magnetic characteristics and geochemical characteristics to the Tyndall Group. Most importantly, it has a close sedimentological correlation to the Tyndall Group. As part of the Western volcano-sedimentary sequences, correlation with the Tyndall Group places the Bulgobac Falls sequence within the Mount Cripps Subgroup, the upper unit of the Mount Charter Group.

A close correlation with other Mount Cripps Subgroup sequences has also been established, both locally and on a regional basis. The Bulgobac Falls sequence has been shown to be a continuation of the Mount Cripps Subgroup sequence mapped in the Pinnacles area to the south. This has also enabled direct correlation of the syncline, the hinge of which is seen to fold the Mount Cripps Subgroup in the Pinnacles area, to the syncline that incorporates the Bulgobac Falls sequence within its eastern arm.

The Mount Cripps Subgroup is also seen on the Cradle Mountain Link Road. A comparison of the stratigraphies on the Cradle Mountain Link Road and in the Bulgobac Falls area shows distinct differences between the two sequences, but also highlights some important similarities. These may suggest some distinctive characteristics to the Mount Cripps Subgroup, which, while not separating it from the more overwhelming Tyndall Group characteristics, make the northern Tyndall Group correlates identifiable in their own right. The most obvious of these is the thickness of the two sequences, with the Bulgobac Falls sequence having the potential to be the thickest Tyndall Group correlate mapped so far. Both sequences differ from the Tyndall Group type section in the proportion of laminated mudstone and sandstone facies to the other facies. Elsewhere this facies is subordinate to the crystal-rich volcaniclastic sandstone facies, however within the Mount

Cripps Subgroup it is dominant in the Lynchford Member correlate and very common within the Mount Julia Member. This reflects the distal setting of the Bulgobac section.

The base of the Mount Cripps Subgroup has been identified to be the lowest unit of the quartz-poor, crystal-rich volcaniclastic sandstone facies. This is based on the mineralogical and textural characteristics of the unit, its geochemical characteristics and its correlation with the basal unit within the Pinnacles area. Carbonate facies mark the base of the Tyndall group where they are present. The carbonate unit which occurs at the base of the Bulgobac Falls sequence has been correlated with part of the Southwell Subgroup based on its differences from other carbonate units within the Tyndall Group and on similarities to carbonate units found within the Southwell Subgroup.

Chapter 5: Magnetics

5.1 Introduction

Much has been made of the aeromagnetic data for the Bulgobac Falls area, with Kirsner's (1992) inference of a significant fault within the area and correlations of the sequence with the base of the Mount Cripps Subgroup (Poltock, 1993). Two questions arise from these theories if the assertions made in this thesis are valid. First, if the Bulgobac Falls sequence is continuous along strike (cf. Kirsner, 1992), why does the magnetic signature of the rocks vary so dramatically. Second, if the stratigraphic and geochemical identification of the base of the Mount Cripps Subgroup is correct, why does it not have a high magnetic signature in the Bulgobac Falls area. In order to resolve these issues, a detailed petrographic study of heavy mineral separates was carried out.

5.2 Methods

Representative samples from the magnetic and non-magnetic units were selected. In particular samples with low magnetic susceptibility (to the north) which had a high magnetic signature along strike (to the south) and from the non-magnetic unit identified as the base of the Mount Cripps Subgroup in this area were selected for investigation. Samples were trimmed of weathered surfaces and crushed to <3mm sized grains. Crushed samples were sent to Analabs for heavy mineral separation. The returned heavy minerals were then sieved to .25mm, and the coarser grained material discarded. The magnetic fraction of the sample was separated using a rare earth magnet in a plastic slip. The magnet was passed over the sample at a height of approximately 5mm, and the magnetic fraction of the sample shaken from the plastic slip after removal of the magnet. The magnetic and non-magnetic fractions were then weighed and grain mounts prepared.

Point counting was completed by recording the number of each mineral type seen within a field of view. The slide was then moved by hand in a straight line along the length of the slide such that the next field of view was immediately adjacent to the previous one. This was continued until approximately 200 grains were counted.

5.3 Results and Discussion

5.3.1 The Base of the Mount Cripps Subgroup

Table 5.1 presents the results from the point counting. The sample taken from the unit at the proposed base of the Mount Cripps Subgroup (P33) contained no magnetic fraction. No magnetite or ilmenite was found in this sample and only a trace of hematite. The count for anatase was high (17%), although its actual proportion of the total count was masked by an extremely high chlorite count (66%). The anatase count was almost nine times higher than tourmaline (2%), the next most abundant mineral.

If the chlorite count is ignored, the relatively high anatase count may be indicative of a previous high concentration of Fe-Ti oxides. The whole rock geochemical analysis for this rock shows that it his an overall iron content consistent with other Mt Cripps Subgroup samples with moderately high magnetic signatures (eg P39,P40 and P44), but well below that of the most highly magnetic rocks (eg L9 and P60). Only iron-rich chlorite will sink during heavy mineral separation, so the abundance of chlorite in this sample suggests it has an iron-rich composition. Since the bulk rock composition is not depleted, the most likely scenario is that the Fe has been shifted from Fe-Ti oxide to chlorite during metamorphism or another alteration process

6.3.2 The Along Strike Magnetic Anomaly

The southern samples came from units that have a large range of magnetic susceptibility (Fig. 5.1). All samples had a similar magnetite content in magnetic separates but the most magnetic sample (P54) had a considerably higher overall percentage of heavy minerals indicating a higher overall percentage of magnetite within the rock (Table 5.1). Conversely, the rock with the lowest magnetic signature (P42) has the lowest percentage weight of sinks.

Both the northern samples have magnetic susceptibility readings under 200×10^{-5}nT, which is similar to that of P42. P50 has the lowest percentage of magnetite, but a concentration of heavy minerals that is at least double the other samples from both regions, with the exception of P54. P70 has a similar magnetite percentage and heavy mineral concentration to the southern samples except P54.

	Sample						
	NP44	NP54	NP50	NP70	NP39	NP42	P33
Zircon (E)	3	4	3	2	12	3	
Zircon (R)	2	5	3	3	13	7	2
Chlorite	14	29	24	5	77	20	134
Tourmaline	10	14	7	4	8	14	4
Apatite	11	78	68	17		20	1
Rutile	2			1		8	
Pyrite	10			1	11		2
Goethite	82		27	68	3	24	2
Anatase	8	63	11	9	23	10	35
Illmenite	36		49	111	28	60	
Magnetite							
Hematite	17	12	8	39	10	34	2
Other	21	14	10		34	13	22
Total	216	219	210	260	219	213	204
Weights gms							
Non-mag. Fraction	0.09308	2.97734	0.31612	0.2363	0.1176	0.07815	0.8088

	MP44	MP54	MP50	MP70	MP39	MP42
Zircon (E)						
Zircon (R)						1
Chlorite	6	28	41	9	28	10
Tourmaline	2	7		2		3
Apatite	8	24	10			2
Rutile				1		
Pyrite	11		5	5		28
Goethite	11	3	17	10		3
Anatase	3		11	5		
Illmenite						
Magnetite	161	173	124	173	181	159
Hematite				2		
Other	2	12	9	3	14	5
Total	204	247	217	210	223	211
Total count	420	466	427	470	442	424
part. altered magnte	33	0	54	81	94	87
Weights gms						
Magnetic fraction	0.16036	1.44695	0.20561	0.17021	0.2937	0.05257
Total	0.25344	4.42429	0.52173	0.40651	0.4113	0.13072

Table 5.1: Results from point counting and weights of magnetic and non-magnetic fractions of samples. Samples identified by the prefix N are the non-magnetic fraction. M prefix designates magnetic fraction.

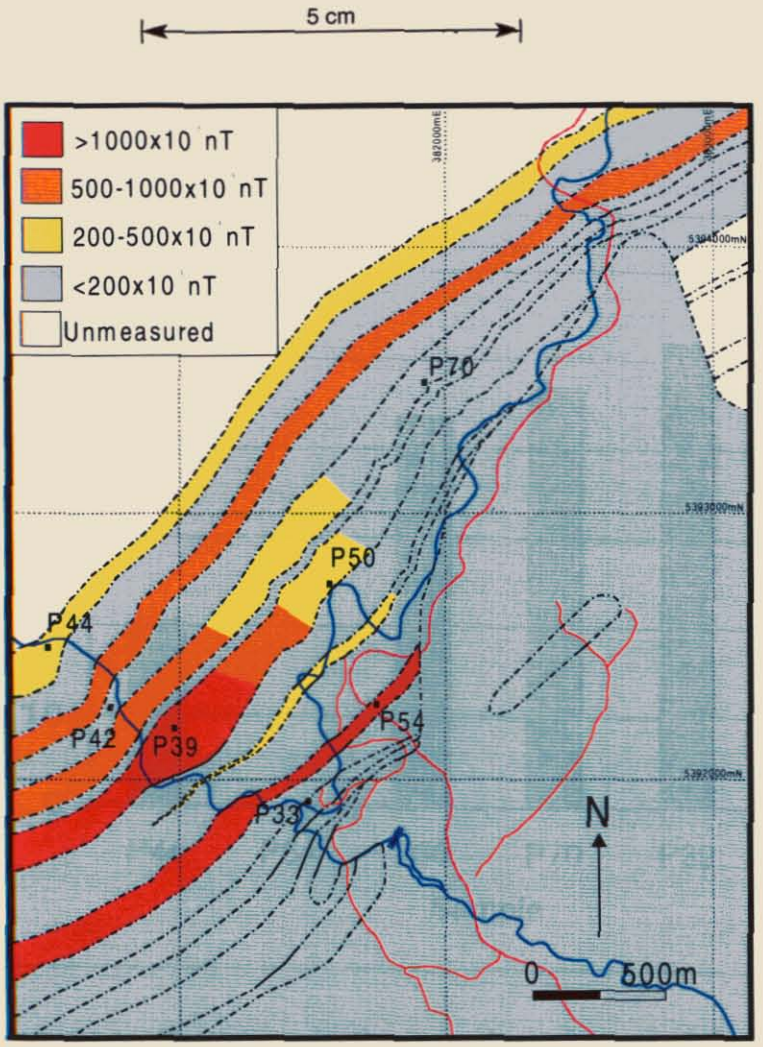

Figure 5.1: Schematic drawing of magnetic susceptibility readings across the Bulgobac Falls area, showing sample locations. Lithological units are as indicated on main map. Along strike magnetic changes are based on isolated outcrop readings and variations are not necessarily sharp. The boundaries are schematic.

	Southern Samples				Northern Samples	
Sample	P39	P42	P44	P54	P50	P70
% sinks	0.54	0.17	0.43	34.81	1	0.3
% magnetite	40.95	37.5	38.33	37.12	29.04	36.81
% altered mag.	51.93	54.72	20.5	0	43.54	46.82

Table 5.2: Comparison of the concentrations of components of the heavy mineral separates from the northern (low magnetic susceptibility) and southern (high magnetic susceptibility regions of the Bulgobac Falls area. % sinks is the percentage of heavy minerals that separated from the original sample. % magnetite is the percentage of magnetite grains in the total count from both the magnetic and non-magnetic fractions of the sample. % altered magnetite is the percentage of magnetite grains that showed evidence of alteration to hematite.

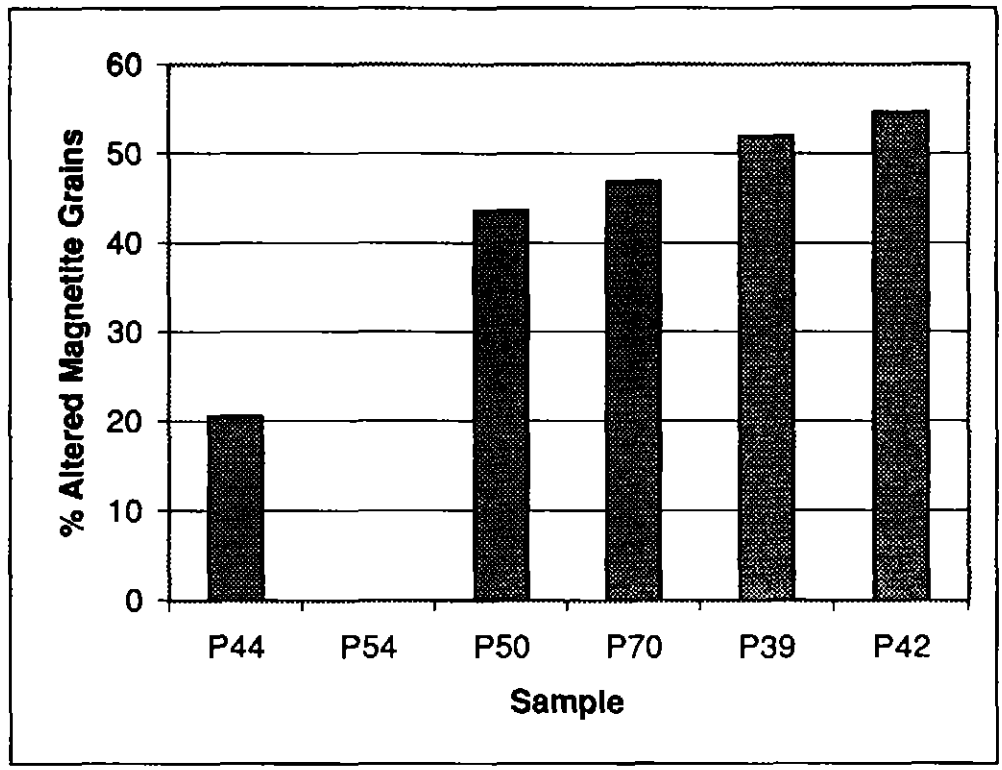

Figure 5.2: The percentage of magnetite grains showing evidence of alteration to hematite

When a comparison is made between the percentages of magnetite grains which show rims that have been altered to hematite a more obvious trend emerges (Fig. 5.2). P54 and P44 have less than half the magnetite grains with alteration rims of the other samples. P39, P44 and P54 are all from highly magnetic units, however P39 is a highly weathered example of this unit. P42 is from the interbedded mudstone and medium to coarse sandstone facies, which has a low magnetic susceptibility and has the lowest concentration of heavy minerals, suggesting a difference in sediment source overall. If these two results are discounted, Figure 5.2 suggests the northern samples have undergone more intense processes of alteration that have reduced the magnetite content of the unit.

Chapter 6: Summary and Conclusions

6.1 Introduction

The stratigraphy of the Mount Read Volcanics is complex and not well understood. Original stratigraphic relationships were complicated and have become even more difficult to determine due to subsequent deformation, complicated faulting and the intermittent nature of the outcrop. Correlations throughout the Mount Read Volcanics belt are difficult and have led to much controversy. An example of this is seen within this thesis in which the Tyndall Group correlate for the northern Mount Read Volcanics is a subgroup (Mt. Cripps Subgroup) of another group (Mt. Charter Group). Unravelling the stratigraphy of the Mount Read Volcanics is economically important because of the potential for ore bodies to be restricted to particular stratigraphic horizons. Scientifically it is important as it will lead to a clearer understanding of the nature of the depositional environments of the Mount Read Volcanics and the subsequent geological history of the area.

The main focus of this thesis has been to determine the stratigraphic sequence within the Bulgobac Falls area and to place it within the overall context of the Mount Read Volcanics. This was achieved by correlating it to other stratigraphic sequences, in particular, the Tyndall Group and the Mount Charter Group. A correlation was also made to local stratigraphic sequences to develop a more detailed picture of the overall pattern of the local geology. In addition, the previous structural model for the area, based on aeromagnetic anomalies, which were tested by field observations.

6.2 Summary

6.2.1 Bulgobac Falls

Stratigraphy

A large quartz-feldspar porphyry body bounds the eastern side of the Bulgobac Falls area. Its cross-cutting relationship with the stratigraphy determines that it is intrusive, although the timing of the intrusion is not clear. Overlying this, five sedimentary lithofacies were identified: a calcareous volcaniclastic sandstone; a mudstone with fine sandstone layers; an

interbedded mudstone and medium to coarse sandstone; a quartz-poor crystal-rich volcaniclastic sandstone and a quartz-rich, crystal-rich volcaniclastic sandstone. These sequences were deposited by low- and high-density turbidity currents or debris flows in a subaqueous environment below storm wave base. Syn-eruptive deposition is inferred based on the high proportion of euhedral and fragmented volcanic crystals found in the sandstones.

A calcareous volcaniclastic sandstone is the basal unit within the area. The upper portion of this unit contains bouldery calcite clasts, some of which are fossiliferous, bearing ostracods and trilobites from the late Middle Cambrian. Overlying this are repeated sequences of the other facies described. The overall trend upwards through the stratigraphy is for the crystal-rich volcaniclastic sandstones to have an increased proportion of quartz crystals and a reduction of pyroxene crystals. Within the lower portion of the stratigraphy, mudstone bearing facies are dominant. These are still prevalent higher within the stratigraphy, but the quartz-rich, crystal-rich volcaniclastic sandstone facies dominate the upper stratigraphy.

Structure

The sequence dips steeply to the west and is upright, based on the upward fining turbidites. Interpretation of relationship of cleavage to bedding indicates that the area forms the eastern arm of a syncline, which is correlated to the syncline hinge mapped in the Pinnacles area by McKibben (1993). The rocks in this area have been subject to at least two phases of deformation which are equated to D2 and D4 of the Tabberabberan Orogeny producing NNE and NW trending folds and weak axial planar cleavage (Seymour and Calver, 1995). No evidence of significant faulting was found and, in particular no evidence could be found for the structural model put forward by Kirsner (1992).

6.2.2 Tyndall Group Correlation

The Bulgobac Falls sequence can be clearly correlated to the Comstock Formation, the lower of the two Tyndall Group formations. Crystal-rich volcaniclastic sandstones are the dominant facies within the Comstock Formation, which also includes laminated mudstones and sandstones, volcaniclastic lithic breccias, carbonates, welded ignimbrites and coherent rhyolites (White, 1996).

The Comstock Formation is divided into a lower Lynchford Member and an upper Mount Julia Member, based in part on the Mount Julia Member having the quartz-rich, crystal-rich volcaniclastic sandstone and being poor in the laminated mudstone facies (White, 1996). The Bulgobac Falls sequence can be divided in a similar manner to the Comstock Formation. The lower portion of the Bulgobac Falls sequence contains the quartz-poor, crystal-rich volcaniclastic sandstone and a higher proportion of mudstone bearing facies and is here described as a Lynchford Member correlate. The upper portion of the sequence contains the quartz-rich, crystal-rich volcaniclastic sandstone and is reduced in mudstone bearing facies. This trend provides a ready correlation with the Mount Julia Member.

The Bulgobac Falls sequence differs from Tyndall Group in that it has a much higher proportion of mudstone bearing facies. Mudstone bearing facies dominate the sequence within the Lynchford Member correlate. This is unlike other examples of the Lynchford Member where mudstone bearing facies are usually less dominant. The exception being very thin Lynchford Member sequences where the crystal-rich sandstones and lithic breccias tend to be absent and the mudstone bearing facies may be the only facies present. Within the Mount Julia Member the mudstone facies are usually minor. However within the Mount Julia Member correlate at Bulgobac Falls, the mudstone facies are significant although less prevalent than in the Lynchford Member correlate. The welded ignimbrites and coherent rhyolites are also missing from the Mount Julia Member, however the full extent of this member was not mapped, so they may occur higher in the stratigraphy.

A strong correlation between the Bulgobac Falls sequence and the Tyndall Group has also been established based on whole rock geochemical analysis. These analysis showed similar trends in the chemical composition of the rocks in the Bulgobac Falls area to those already identified by Berry *et al* (1997) as unique trends in the composition of Lynchford Member rocks. These trends are the result of significant input from tholeiitic source rocks, a feature not found in other Mount Read Volcanics rocks.

The base of the Tyndall Group correlate is identified as the first of the quartz-poor, crystal-rich volcaniclastic sandstones. This identification is based on its lithological and geochemical similarity to other Lynchford Member units and to the overlying Lynchford Member correlates in the area.

6.2.3 Mt Charter Group Correlation

At the base of the Lynchford Member a fossiliferous carbonate facies, with Mid-Late Cambrian trilobites at its base is sometimes found. The calcareous volcaniclastic sandstone at the base of the Bulgobac Falls sequence does not provide a good correlation with Lynchford Member however as the Lynchford Member carbonates are massive rather than clasts of carbonate within a sandstone. It does however, lead to a correlation between the Bulgobac Falls sequence and the Mount Charter Group.

The uppermost portion of the Mount Charter Group contains the Southwell Subgroup and the overlying Mount Cripps Subgroup. The Southwell Subgroup includes beds with limestone clasts some of which contain fossil trilobites. The combination of a Tyndall Group correlate overlying a unit which can be correlated to the Southwell Subgroup, provides an excellent correlation to the Mount Charter Group.

The Bulgobac Falls sequence is linked to the sedimentary sequence mapped in the Pinnacles area as Southwell Subgroup, with overlying Mt. Cripps Subgroup (McKibben, 1993). Aeromagnetic mapping shows a magnetic high trending along strike which links a magnetic unit in the Bulgobac Falls area to a lithologically and magnetically similar unit in the Pinnacles area. A second magnetically high unit which is marks the base of Mount Cripps Subgroup in the Pinnacles area can be linked to the unit previously identified as the base of the Mount Cripps Subgroup in the Bulgobac Falls area. The aeromagnetic data shows this unit loses its magnetic signature between the two regions. This local correlation provides further support for placing the Bulgobac Falls sequence within the Mount Charter Group.

6.2.4 Magnetic Anomalies

Kirsner's (1992) model for a significant NW trending fault disrupting the stratigraphy was not supported by field mapping or geochemical analysis. The magnetic low that occurs along strike from highly magnetic beds are explained by alteration of magnetite within the magnetic units to hematite. Magnetic units had low levels of altered magnetite grains, while less magnetic units had significantly higher counts of magnetite grains with hematite rims.

The correlation of the non-magnetic crystal-rich volcaniclastic sandstone to the base of the Mount Cripps Subgroup when previous studies had given the expectation that this bed should be highly magnetic (McKibben, 1993; White and McPhie, 1996) can be similarly justified. Evidence is presented that suggests this bed contained a high proportion of titanomagnetite which has been altered to anatase.

6.3 Conclusions

The sequence described for the Bulgobac Falls area is clearly part of the Mount Charter Group, specifically the uppermost part of the Southwell Subgroup, and the lower units of the Mount Cripps Subgroup, a correlate of the Tyndall Group. The base of the Mount Cripps Subgroup is the first of the quartz-poor, crystal-rich volcaniclastic sandstones in the area. Previous studies have suggested the Tyndall Group and its correlates can be identified by their highly magnetic signature. This study shows that while this may be a good guide to the presence of the Tyndall Group and its correlates, the magnetic signature of the rocks can be affected by alteration and should not be used to exclude individual units without other supporting evidence.

The thickest sequences of Tyndall Group rocks described so far have both come from the Mount Cripps Subgroup at Bulgobac Falls and Cradle Mountain Link Road. Further correlations between the two Mount Cripps Subgroup stratigraphies described at these locations are the significantly higher presence of the laminated mudstone and sandstone facies and thinner beds of the coarser grained mass flow deposits. This may be an indication of a common feature to the Mount Cripps Subgroup and is likely be an the result of a differing depositional environment for these rocks from Tyndall Group rocks. The common relative thinness of the mass flow beds within the Mount Cripps Subgroup could indicate the depositional environment is more distant from the source of the sediments and that these beds represent, or are nearer to, the leading edges of the mass flows. The greater presence of finer grained material supports this, as it could represent the outer limits of high-density turbidity flows, as the finer material is carried further by the energy of the system.

A second possible reason for these features could be that it represents an environment that is further from the source of energy that initiated the turbidity flow. If these deposits are

syn-eruptive as has been suggested, the turbidity currents would have been initiated by eruptions or earthquakes, probably associated with the volcanic activity. If the depositional environment for the Mount Cripps Subgroup was further from the areas of volcanic activity, there would be less energy supplied to the system to initiate the currents, the currents would carry less coarse material and more fine material. This would lead to thinner beds of coarse grained material from high-density turbidity currents and thicker sequences resulting from low-density turbidity currents. If this was the case, it would suggest that this part of the basin was further from the volcanic sources than it is now.

This work has not fully determined the extent of the Mount Cripps Subgroup in this area. The aeromagnetic data suggests that it continues further west, but as is suggested here, is not repeated far beyond the hinge of the syncline. The absence of a western repetition of the highly magnetic ridges that represent the base of the Mount Cripps Subgroup to the east suggests that the Rosebery Fault may have removed much of the western limb of the syncline. This region includes probable Owen-type conglomerates (Corbett *et al*, 1997) which would be consistent with reverse movement along the Rosebery Fault bringing the Mount Cripps Subgroup in to lateral contact with overlying Owen Conglomerate. Future mapping within the area should be able to clearly resolve the full extent of the syncline and the existence and impact of the Rosebery Fault in this area.

References

Baille P. (1989). Stratigraphy, Sedimentology and Structural Setting of the Cambrian Sticht Range Formation, western Tasmania. Geol Surv. Tas. Bull. **65**: 34pp

Banks M. R. and Solomon M. (1961). Cambrian Succession in West Tasmania. Aust J Sci **23**: 337

Berry R. F. and Crawford A. J. (1988). The tectonic Significance of Cambrian Allochthonous Mafic-ultramafic Complexes in Tasmania. Aust. J. Earth Sciences, **35**: 523-533.

Berry R. F., Selley D., White M. J. and Meffre S. (1997). Lithogeochemistry. **In**: The Structure and Mineralisation of Western Tasmania. Amira Project P291A, Final Report. Centre for Ore Deposit and Exploration Studies, University of Tasmania, Hobart. 33-58.

Campana B., King D. and McKenna D. (1960). Unconformable Units of the Cambrian Succession of West Tasmania. Aust J Sci. **22**: 352-353.

Cas R. A. F. and Wright J. V. (1987). Volcanic Successions: Modern and ancient. A Geological Approach to Processes, Products and Successions. Allen and Unwin, London.

Collins P. L. F. (1980) Geology of the Pinnacles – Que River Area. Map Accompanying Mackintosh Explanatory Report. Dept of Mines. Tasmania. Hobart.

Compton R. R. (1985). Geology in the Field. Wiley and Sons.

Corbett K. D. (1992). Stratigraphic-Volcanic Setting of Massive Sulfide Deposits in the Cambrian Mount Read Volcanics, Tasmania. Economic Geology, **87**: 564-586.

Corbett K. D. (1992). Stratigraphic-Volcanic Setting of Massive Sulphide Deposits in the Cambrian Mount Read Volcanics, Tasmania. Economic Geology **87**: 564-586.

Corbett K. D. and Komyshan P. (1989). Geology of the Hellyer – Mt. Charter Area. Geol. Rep. Mt Read Volc. Proj., Tasm. **1**. Tasmania Division of Mines and Mineral Resources.

Corbett K. D. and Lees T. C. (1987). Stratigraphic and Structural Relationships and Evidence for Cambrian Deformation at the Western Margin of the Mt. Read Volcanics, Tasmania. Aust. J. Earth Sciences, **34**: 45-67.

Corbett K. D., Banks M. R. and Jago J. B. (1972). Plate Tectonics and the Lower Palaeozoic of Tasmania. Nature 240: 9-11.

Corbett K. D., Berry R. F. and Selley D. (1997). Stratigraphic Correlation and Basin Analysis. **In**: The Structure and Mineralisation of Western Tasmania. Amira Project P291A, Final Report. Centre for Ore Deposit and Exploration Studies, University of Tasmania, Hobart. 59-67

Corbett K. D. and Turner N. J. (1989). Early Palaeozoic Deformation and Tectonics. **In**: Burrett C. F. and Martin E. L. (eds). Geology and Mineral Resources of Tasmania. Geol. Soc. Aust. Spec. Pub. 15: 154-181.

Crawford A. J. and Berry R. F. (1992). tectonic Implications of the Late Proterozoic-Early Palaeozoic Igneous rock associations in Western Tasmania. Tectnophysics, **214**: 37-56.

Deer W. A., Howie R. A. and Zussman J. (1992). An Introduction to Rock Forming Minerals. 2ed. Longman Group, Hong Kong.

Green D. C. (1995). ETA 384 Bulgobac – Notes on Geology and Exploration. Unpub Mineral Resources Tasmania. Hobart.

Jago J. B. and McNeill A. W. (1997). A Late Middle Cambrian Shallow-water Trilobite Fauna from the Mt. Read Volcanics, Northwestern Tasmania. Papers and Proceedings of the Royal Society of Tasmania **131**: 85-90.

Jago J. B., Reid K. O., Quilty P.G., Green G. R. and Daily B. (1972). Fossiliferous Cambrian Limestone from within the Mount Read Volcanics, Mt Lyell Mine Area, Tasmania. J Geological Soc. Australia, **19** (3): 379-382

Kirsner L. W. (1992) EL 2/90 Boco EL 8/90 North Pinnacles Exploration Report for the Period 11/10/90-29/2/92. Unpub. Pasminco Exploration. Burnie.

Kuenen P.H. H. and Migliorini C. I. (1950). Turbidity Currents as a Cause of Graded Bedding J. Geol. **58**: 91-127.

Leeder M. R. (1982). Sedimentary Processes and Products. Allen and Unwin, London.

Lowe D. R. (1982). Sediment Gravity Flows: II. Depositional Models with Special Reference to the Deposits of High-Density Turbidity Currents. J Sed Petrol **52**: 279-297.

MacDonald G. (1991) The Comstock Chert: Implications for the Mt. Lyell Geology. Unpub. BSc (Hons) thesis. University of Tasmania, Hobart.

McClay K. R. (1987). The Mapping of Geological Structures. John Wiley and Sons, Chichester.

McKibben J. A. J. (1993). The Geology and Geochemistry of the North Pinnacles Ridge, Western Tasmania. Unpub. BSc. Honours thesis. University of Tasmania, Hobart.

McNeill A. W. and Corbett K. D. (1992). Geology and Mineralisation of the Mt. Murchison Area. Mt Read Volcanics Proj. Geological Report **3** Tasmania Division of Mines and Mineral Resources.

McPhie J. and Allen R. L. (1992). Facies Architecture of Mineralized Submarine Volcanic Sequences: Cambrian Mount Read Volcanics, Western Tasmania. Economic Geology **87**: 587-596.

McPhie J., Doyle M. and Allen R. (1993). Volcanic Textures: A Guide to the Interpretation of Textures in Volcanic Rocks. Centre for Ore deposit and Exploration Studies. Hobart.

Pemberton J. and Corbett K. D. (1992). Stratigraphic Facies Associations and Relationship to Mineralisation in the Mount Read Volcanics. Tasmania: An Island of Potential. Geol Soc Bull. **70**: 167-176.

Pemberton, J., Vicary M. J., Corbett K. D. (1991). Geology of the Cradle Mountain Link Road – Mt. Tor Area. Geol. Rep. Mt. Read Volc. Proj. Tasm. **4**. Tasmania Division of Mines and Mineral Resources.

Poltock R. A. (1993). EL 2/90 Boco EL 8/90 North Pinnacles Exploration Report for the Period 29/2/92-6/5/93. Unpub. Pasminco Exploration. Burnie

Polya D. A., Solomon M., Eastoe C. J. and Walshe J. L. (1986). The Murchison Gorge, Tasmania – A Possible Cross-section Through a Cambrian Massive Sulphide System. Economic Geology, **81**: 1341-1355.

Seymour D. B. (1980). The Tabberabberan Orogeny in northwest Tasmania. PhD. Thesis, University of Tasmania.

Seymour D. B. and Calver C. R. (1995). Explanatory Notes for the Time-Space Diagram and Stratotectonic Elements Map of Tasmania. *Tasgo NGMA Project, Sub-project 1: Geological Synthesis. Tasmanian Geological Survey,* **Record 1995/01**.

Taylor S. R. and McClennan S. M. (1958). The Continental Crust: its Composition and Evolution. Blackwell Sci Pub. Oxford

White M. J. (1996). The Stratigraphy, Volcanology and Sedimentology of the Cambrian Tyndall Group, Mount Read Volcanics, Western Tasmania. Unpub. PhD thesis. University of Tasmania, Hobart.

White M. J. and McPhie J. (1996). Stratigraphy and Palaeovolcanology of the Cambrian Tyndall Group, Mt. Read Volcanics, western Tasmania. Aust. J. Earth Sciences **43**: 147-159.

Williams E. (1989). Summary and Synthesis. **In**: Burrett C. F. and Martin E. L. (eds). Geology and Mineral Resources of Tasmania. Geol. Soc. Aust. Spec. Pub. 15: 468-499.

Williams E., McClenaghan M. P. and Collins P. L. F. (1989). Mid-Palaeozoic Deformation, Granitoids and Ore Deposits *in*: Burrett, C. F. and Martin, E. L. (eds.). Geology and Mineral Resources of Tasmania. *Special Publication Geological Society of Australia* 15: 238-292.

Williams H. and McBirney A. R. (1979). Volcanology. Freeman Cooper and Co. San Francisco.

Wilson D. R. (1989). Geological Report 64-23-9. Hydro Electric Commission Tasmania. Hobart.

Wray J. L. (1977). Calcareous Algae. Elsevier Scientific Publishing Co. Amsterdam.

APPENDIX A

Structural Data

BEDDING		
Strike	Dip	Sense
20	60	W
20	30	W
20	55	W
30	52	W
20	55	W
20	65	W
30	60	W
30	45	W
40	50	W
40	42	W
35	58	W
38	60	W
40	34	W
50	45	W
50	45	W
40	52	W
15	90	W
10	75	W
9	85	W
10	66	W
55	56	W
30	58	W
35	78	W
45	55	W
35	78	W
28	63	W
40	63	W
30	80	W
25	68	W
40	78	W
25	80	W
28	75	W
28	80	W
25	73	W
25	78	W
28	80	W
24	78	W
18	70	W
25	80	W
40	53	W
25	77	W
35	55	W
60	47	W
25	65	W
10	47	W
17	58	W
20	62	W
38	52	W
35	48	W

CLEAVAGE		
Strike	Dip	Sense
20	90	W
24	56	W
30	70	W
65	90	W
40	90	W
130	85	N
45	75	W
30	90	W
35	90	W
60	90	W
3	72	W
345	88	W
46	64	W
0	90	W
70	50	W
146	56	W
10	70	W

FOLDS	
Trend	Plunge
295	43
280	40
280	30
30	32
20	21
30	35
295	43
7	30
0	30
350	27
295	43
280	40
280	30

APPENDIX B

XRF Data

BUXTONMO

Traces with ScMo Tube		MOCOMP3 program		5 Sept.1997	Phil Robinson/KatieMcGoldrick			
Ident	**Y**	**Rb**	**Th**	**Pb**	**Ni**	**Zn**	**Cu**	**As**
TASGRAN1(8)	35.6	251.8	17.1	26.2	2.9	35.6	2.2	<3
TASBAS	20.8	16.9	5.1	4.4	149.4	117.7	63.4	<3
ig.COMSiO2	<1	<1	<1.5	<1.5	<1	<1	<1	<3
GXR2/527	18.4	78.6	9	687.1	17.8	536.3	76.7	26.3
GXR4/541	15.5	145	31.9	46	37.9	75	6266.1	103
GSS5	23.8	118.5	42.9	569.8	43.6	501.2	141.1	409.9
L9	28	57	4	21	67	461	97	18
P16	32	146	14	29	23	92	3	4
P20	21	84	10	33	2	92	3	5
P33	27	54	6	25	10	188	7	7
P38	39	77	15	63	24	93	2	<3
P39	23	185	2	337	12	709	20	6
P40	40	34	4	267	13	631	69	5
P42	24	50	9	3	15	120	2	4
P43	26	30	8	8	36	99	11	<3
P44	31	54	9	16	20	205	17	7
P51	24	65	7	63	11	324	4	3
P52	45	173	20	24	25	82	18	15
P60	38	63	5	29	39	227	20	10
P67	50	90	11	30	104	401	25	<3
P68	44	37	5	13	13	91	8	6
P70	21	67	8	5	39	140	4	4
TASBAS	20.3	16.5	4.5	5.3	149.1	117.4	64.6	<3
TASGRAN1(8)	35.4	250.8	17	26.3	3.2	35.7	2.3	<3
						not requested	not requested	not requested

Buxton(AU)

Ident	Nb	Zr	Sr	Ba	Sc	V	Cr	La	Ce	Nd
2000SR(1)	1.2	-0.3	1980.8	4.7	-0.5	2.5	396.3	<2	<4	<2
AGV1	13.4	230.1	663.8	1177.9	14.6	119	10.3	39.1	66.7	33.8
ENDV	5.5	108.9	161.9	69.6	41.8	281.8	313	6.6	13.4	10.8
ENDV(2)	6.6	109.8	161.8	66.9	41.3	283.4	315	10.5(cont.?)	15.8	11.9
ig.COMSiO2	<1	<1	<1	<4	<2	<1.5	<1	5(cont.)	<4	<2
RGM1	8.7	231.4	103.4	806.3	4.6	11.6	3.5	23.4	45.1	21.7
RSES#8	0.5	11.1	137.6	51.1	43.6	305.3	55	3.2(cont.?)	3.4	1.2
TASBAS	54.1	256.9	1015.2	199.7	13.8	156.2	188.1	44.5	86.8	41.6
TASBAS	54.2	257.2	1013	201.1	13.9	157.1	187.6	43.2	86.3	40
TASGRAN1(8)	13.2	158.1	145.6	460.2	5.7	24.3	9.5	38.2	80.7	35.9
TASGRAN1(8)	13.6	157.8	145.9	461.7	6.5	24.4	9.2	39.6	80.2	37.3
Samples										
Ident	**Nb**	**Zr**	**Sr**	**Ba**	**Sc**	**V**	**Cr**	**La**	**Ce**	**Nd**
[PB]L9	23	254	286	689	45	992	130	33	62	32
[PB]P16	14	241	14	590	12	45	30	42	85	37
[PB]P20	10	180	167	814	10	20	3	27	58	28
[PB]P33	11	282	691	2048	20	103	26	25	56	29
[PB]P38	14	283	156	484	13	84	36	50	104	51
[PB]P39	9	210	130	4049	18	107	30	32	47	32
[PB]P40	13	299	368	593	27	176	37	24	60	37
[PB]P42	11	197	362	378	19	144	42	33	68	27
[PB]P43	11	194	173	1014	14	82	153	27	59	29
[PB]P44	11	171	306	1460	19	161	50	34	66	33
[PB]P51	11	266	223	1193	19	103	27	14	53	17
[PB]P52	13	193	101	1706	11	67	34	50	99	47
[PB]P60	14	144	121	1011	47	366	119	50	49	51
[PB]P67	13	212	47	580	18	94	129	101	170	78
[PB]P68	13	316	417	631	29	183	42	29	71	43
[PB]P70	10	230	62	623	15	122	323	40	78	37
5 Sept.1997	Phil Robinson/KatieMcGoldrick			AU1 program	University of Tasmania		XRF			

BuxtonMajors

Ident	SIO2	TIO2	AI2O3	Fe2O3	MnO	MgO	CaO	Na2O	K2O	P2O5	BaO	Loss Inc. S-	Sum	S
BLANK(3/9)N	89.92	0	0.01	10.04	0	0.01	0	0	0	0	0.01	0	99.99	<0.01
TASDIOR(3/9)N	65.19	0.61	15.05	5.62	0.11	3.07	4.84	1.96	2.24	0.17	0.07	1.35	100.28	0.02
TASGRAN(3/9)N	73.04	0.29	13.69	2.28	0.04	0.7	1.85	2.79	4.64	0.12	0.06	0.73	100.23	<0.01
L9	42.26	4.18	14.19	24.32	0.55	2.93	2.46	2.16	1.67	0.47	0.08	4.16	99.43	0.44
P16	72.1	0.33	12.96	4.78	0.08	2.05	0.25	0.02	3.55	0.06	0.07	3.38	99.63	0.14
P20	42.92	0.27	12.63	1.62	0.11	2.4	18.29	1.16	2.32	0.09	0.09	17.71	99.61	0.07
P33	62.57	0.65	16.07	6.46	0.19	2.42	2.45	3.75	1.8	0.13	0.23	2.83	99.55	<0.01
P38	67.24	0.46	15.79	4.43	0.07	2.64	0.28	3.9	2.03	0.19	0.05	2.1	99.18	<0.01
P39	58.69	0.61	17.68	6.93	0.24	2.06	0.15	2.46	7.24	0.09	0.42	2.94	99.51	<0.01
P40	61.22	1	15.33	8.13	0.2	2.64	2.99	4.55	1.43	0.16	0.07	2.22	99.94	0.04
P42	61	0.62	16.96	6.8	0.12	3.45	0.59	4.71	1.28	0.18	0.04	3.59	99.34	0.03
P43	71.58	0.52	10.58	5.08	0.1	2.37	2.43	3.32	0.91	0.13	0.11	2.39	99.52	0.01
P44	62.73	0.83	14.47	8.24	0.19	2.73	0.98	4.25	2.53	0.28	0.16	2.39	99.78	<0.01
P51	62.41	0.66	17.44	5.56	0.25	1.93	0.27	5.91	1.95	0.12	0.13	2.96	99.59	<0.01
P52	65.37	0.34	16.86	4.11	0.04	1.9	0.33	1.38	5.68	0.19	0.19	3.44	99.83	0.54
P60	54.36	1.69	14.67	14.81	0.33	4.76	0.39	0.97	1.79	0.21	0.11	6.07	100.16	<0.01
P67	69.04	0.54	12.28	6.85	0.04	3.03	0.14	0.08	2.12	0.11	0.06	5.35	99.64	<0.01
P68	60.12	1.02	15.31	8.73	0.12	1.96	4.72	2.44	1.24	0.15	0.07	4.07	99.95	<0.01
P70	75.51	0.62	9.76	5.64	0.07	2.24	0.17	1.28	1.89	0.12	0.07	2.76	100.13	<0.01
TASDIOR[PB]	65.07	0.6	14.92	5.62	0.11	3.05	4.81	1.94	2.23	0.16	0.07	1.35	99.93	0.02
TASGRAN[PB]	73.15	0.28	13.71	2.25	0.04	0.7	1.84	2.73	4.61	0.12	0.03	0.73	100.19	<0.01
BLANK[PB]	89.73	0	0.09	10	0	0.01	0	0.02	0	0	0.00	0	99.85	<0.01

APPENDIX C

Outcrop and Data Map

APPENDIX D

Stratigraphic Column from NW of Pinnacles

Provided by A. McNeill

233084

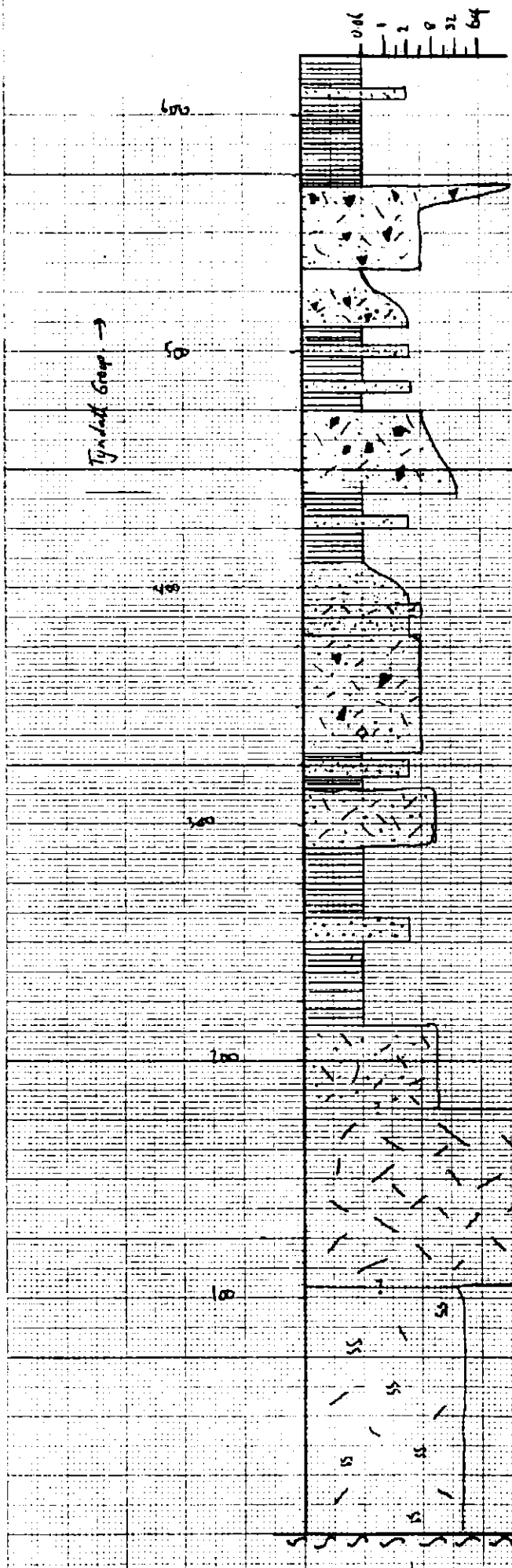

Ltd grey laminated shale and minor sandstone

grey-brown Volcaniclastic sandstone - conglomerate; ? tuff

thin sandstone, ltd & shale-rich sandstone at base

Quartz ± feldspar-phyric, massive, crystal-rich sandstone

Laminated grey shale interbedded with minor thin sandstone

Massive grey- Quartz-feldspar-phyric crystal-rich sandstone

Laminated grey shale with minor thin sandstone

Quartz-feldspar-phyric crystal-rich sandstone; mu

Quartz-feldspar-phyric rhyolite (Pinnacles Rhy

feldspar-phyric ? pumiceous, massive, volcaniclastic

(or is it a lava?)

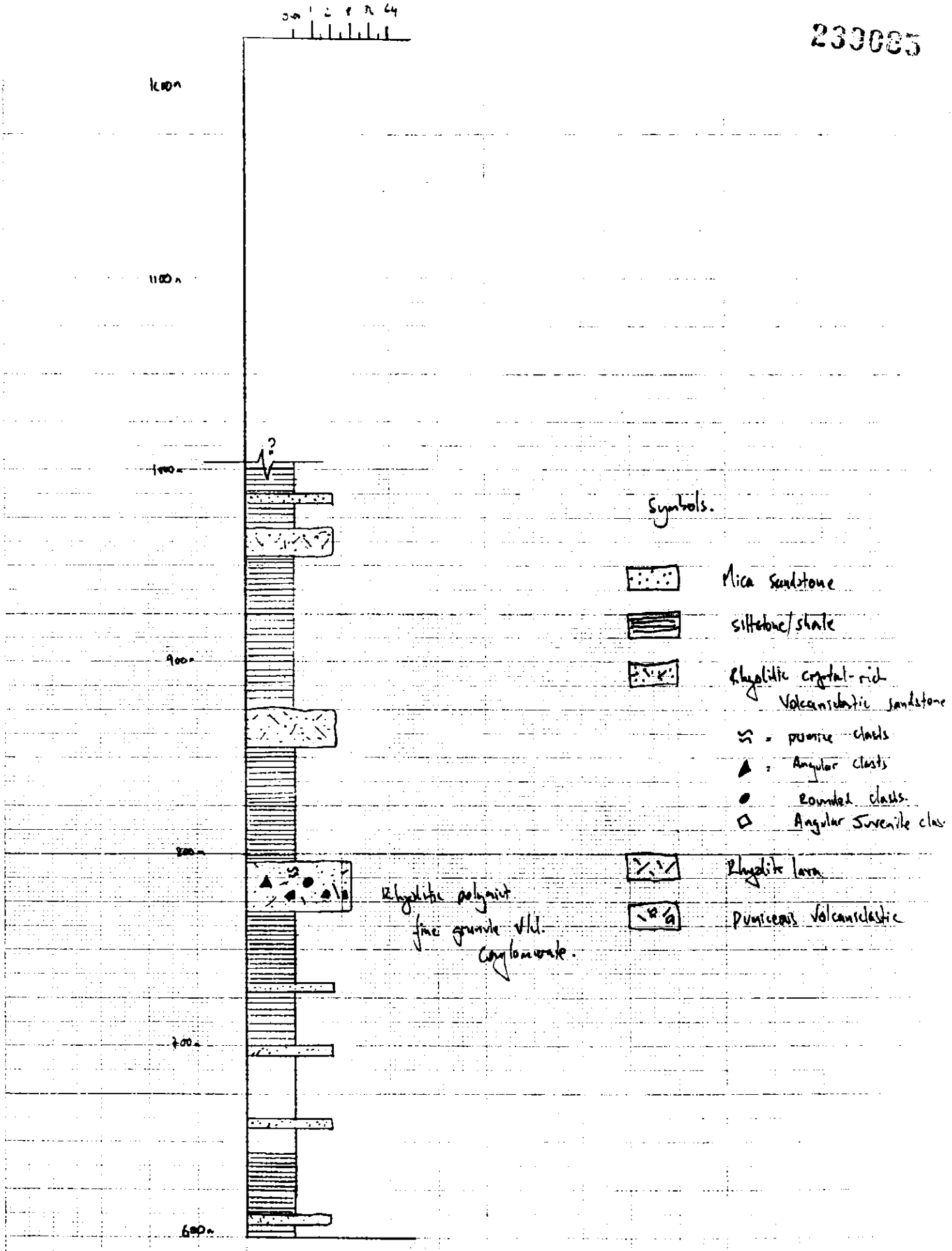
1100 m
1000 m
900 m
800 m
700 m
600 m
?
Symbols.
Mica Sandstone
siltstone/shale
Rhyolitic crystal-rich Volcaniclastic sandstone
: pumice clasts
: Angular clasts
: Rounded clasts.
: Angular Juvenile clas
Rhyolite lava
Pumiceous Volcaniclastic
Rhyolitic polymict fine granule Vfd. Conglomerate.

The Geology of the Bulgobac Falls Area